

THESIS ON NATURAL AND EXACT SCIENCES B55

**Application of ^{13}C and fluorescence labeling in metabolic studies of
Saccharomyces spp.**

ILDAR NISAMEDTINOV

Faculty of Chemical and Material Technology, Department of Food Processing, Chair of Food Technology, Tallinn University of Technology, Tallinn, Estonia

Laboratory of Molecular Genetics, National Institute of Chemical Physics and Biophysics, Tallinn, Estonia

Competence Centre for Food and Fermentation Technologies, Tallinn, Estonia

Dissertation was accepted for the defence of the degree of Doctor of Philosophy in Natural Sciences on microbial physiology and metabolism on September 27, 2006

Opponents:

Dr. Tiina Alamäe, Department of Genetics, Institute of Molecular and Cell Biology, University of Tartu, Estonia

Dr. Heikki Ojamo, Department of Bioprocess Engineering, Technical University of Helsinki, Finland

Commencement: November 17th, 2006 at Tallinn University of Technology

Members of the jury: Dr. Tiina Alamäe, opponent, Dr. Heikki Ojamo, opponent, Prof. Andres Öpik, Prof. Raivo Vokk, Prof. Nigulas Samel, and Prof. Raivo Vilu

Hereby I declare that this doctoral thesis, my original investigation and achievement, submitted for the doctoral degree at Tallinn University of Technology has not been submitted for any degree of examination.

Signature of candidate:

Date:

Copyright: Ildar Nisamedtinov, 2006

ISSN 1406-4723

ISBN 9985-59-655-2

ABSTRACT

In the present doctoral thesis two different labeling techniques were applied for characterization of yeast metabolism: 1) the ^{13}C labeling of brewer's yeast *S. uvarum* W34 on a mixed substrate containing either ^{13}C -[1,2] or ^{13}C -[2] Na-acetate and unlabeled glucose during the low growth rates for visualization of the active metabolic pathways and localization of the enzymatic reactions was carried out in combination with metabolic modeling, and 2) the fluorescence labeling of the small LEA-like heat shock protein Hsp12p using the fusion protein construct Hsp12p:Gfp2p for visualization of the expression of *HSP12* and determination of the yeast cell stress status as a response to different smoothly changing environmental conditions. The continuous culture techniques D-stat and auxo-accelerostat were used in the experiments respectively.

The ^{13}C labeling experiments demonstrated that the intracellular metabolic fluxes can be well predicted on the basis of constructed metabolic network if certain fluxes, such as the specific substrate consumption and product excretion rates as well as the fluxes leading to the biomass components are known. Based on the labeling pattern as well as the absolute and conditional enrichments of proteinogenic amino acids the mitochondrial localization of aspartate and alanine synthesis in the given experimental conditions was identified. The calculated NADPH balance indicated that the NADPH required for the synthesis of biomass components in mitochondria is derived from the reaction catalyzed by malic enzyme.

In the fluorescence labeling experiments the smooth change of two common environmental parameters – temperature and NaCl concentration, known to induce the expression of *HSP12* were applied, and the results were compared with those obtained from the shift-up experiments. It was found for the both parameters that the expression of *HSP12* depends more significantly on the change rate of the stressful environmental condition than on the condition itself. The auxo-accelerostat with smoothly changing stressful environmental parameters using a fusion protein Hsp12p-Gfp2p construct showed to be an efficient tool for studying the response of the yeast metabolism to different industrially or naturally occurring stress conditions.

Keywords: *Saccharomyces* spp., metabolic modeling, ^{13}C labeling, fluorescence labeling, green fluorescent protein, D-stat, auxo-accelerostat, *HSP12*

LIST OF PAPERS

This thesis is based on the following papers and some submitted but yet unpublished results. The papers are referred to by their Roman numerals I-VIII in the text.

- I Drews, M., Kasemets, K., Nisamedtinov, I., Paalme, T. 1998. Continuous cultivation of insect and yeast cells at maximum specific growth rate. *Proceedings of Estonian Academy of Sciences, Chemistry*, 47, p. 175–188.
- II Kasemets, K., Drews, M., Nisamedtinov, I., Adamberg, K., Paalme, T. 2003. Modification of A-stat for the characterization of microorganisms. *Journal of Microbiological Methods*, 55, p. 187–200.
- III Nisamedtinov, I., Adamberg, K. and Paalme, T. 2003. D-stat. *In: S. Sorvari (Ed.), Proceedings of the 1st International Congress on Bioreactor Technology in Cell, Tissue Culture and Biomedical Applications*. Karhukopio OY, Turku, Finland, p. 231-242.
- IV Drews, M., Nisamedtinov, I. and Paalme, T. 2003. Application of quasi-steady-state cultures. *In: S. Sorvari (Ed.), Proceedings of the 1st International Congress on Bioreactor Technology in Cell, Tissue Culture and Biomedical Applications*. Karhukopio OY, Turku, Finland, p. 218-225.
- V Kasemets, K., Nisamedtinov, I., Abner, K. and Paalme, T. 2006. Study of the fermentative growth of *S. cerevisiae* S288C using auxo-accelerostat technique. *In: A. Mendez-Vilas (Ed.), Modern Multidisciplinary Applied Microbiology: Exploiting Microbes and Their Interactions*. Wiley-VCH, Weinheim, p. 756-762.
- VI Paalme, T., Nisamedtinov, I., Laht, T. M., Drews, M. and Pehk, T. 2006. Application of (13)C-[2]- and (13)C-[1,2] acetate in labelling studies of yeast and insect cells. *Antonie Van Leeuwenhoek*, 89, p. 443-457.
- VII Nisamedtinov, I., Lindsey, G., Karreman, R., Orumets, K., Koplmaa, M. and Paalme, T. 2006. Effect of slowly increasing temperature and NaCl concentration on the expression of Hsp12-Gfp2 fusion protein in *Saccharomyces cerevisiae*: an auxo-accelerostat study. *In: S. Sorvari (Ed.), Proceedings of the 2nd International Congress on Bioreactor Technology in Cell, Tissue Culture and Biomedical Applications*. Karhukopio OY, Turku, Finland. *In press*.
- VIII Kasemets, K., Nisamedtinov, I., Laht, T. M., Abner, K. and Paalme, T. Growth characteristics of *Saccharomyces cerevisiae* S288C in changing environmental conditions: auxo-accelerostat study. *Antonie Van Leeuwenhoek*, submitted

The author's contribution in the appended publications

Publication I: I. Nisamedtinov and Kaja Kasemets were responsible for the set-up, operation and data analysis of pH- and CO₂-stat cultivations of yeast.

Publication II: I. Nisamedtinov outlined the research plan for the D-stat experiments with the strains *S. uvarum* W34 and *S. cerevisiae* EC1118, carried out the experiments, sample and data analysis, and was involved in writing the manuscript.

Publication III: I. Nisamedtinov outlined the research plan for the D-stat experiments with *S. uvarum* W34 and *S. cerevisiae* 6267E, carried out all the experiments with these strains and produced majority of the manuscript.

Publication IV: I. Nisamedtinov carried out the yeast cultivation experiments with changing culture volume.

Publication V: I. Nisamedtinov and Kaja Kasemets carried out the auxo-accelerostat experiments.

Publication VI: I. Nisamedtinov and Toomas Paalme outlined the research plan. I. Nisamedtinov carried out all the labeling experiments as well as data analysis from the NMR spectra. Kristo Abner, Toomas Paalme and I. Nisamedtinov were involved in the development of mathematical framework of the metabolic network model. I. Nisamedtinov and Toomas Paalme produced majority of the manuscript.

Publication VII: I. Nisamedtinov outlined the research plan, analysed the results and produced the manuscript.

Publication VIII: I. Nisamedtinov and Kaja Kasemets carried out the auxo-accelerostat experiments. Kaja Kasemets, Toomas Paalme and I. Nisamedtinov produced the manuscript.

TABLE OF CONTENTS

INTRODUCTION	8
LITERATURE REVIEW	9
1.1. <i>Saccharomyces</i> spp.	9
1.2. <i>Saccharomyces uvarum</i>	10
1.3. Metabolism and metabolic network of <i>Saccharomyces</i> spp.	10
1.3.1. Fermentative and respiratory metabolism of <i>Saccharomyces</i> spp.	11
1.3.2. Glucose control mechanisms in <i>Saccharomyces</i> spp.	13
1.3.3. Stress response in <i>Saccharomyces</i> spp. and heat shock proteins	14
1.3.4. High-osmolarity-glycerol pathway in <i>Saccharomyces</i> spp.	15
1.3.5. Amino acid metabolism	16
1.3.5.1 Biosynthesis of amino acids of glutamate family	16
1.3.5.2. Biosynthesis of amino acids of pyruvate family	17
1.3.5.3. Biosynthesis of amino acids of aspartate family	17
1.3.5.4. Biosynthesis of lysine	18
1.3.5.5. Biosynthesis of amino acids of 3-phosphoglycerate family (the serine-glycine-cysteine group)	18
1.3.5.6. Biosynthesis of aromatic amino acids	19
1.3.5.7. Biosynthesis of histidine	19
1.3.6. Metabolism of trehalose and glycogen	20
1.3.7. Metabolism of lipids	22
1.3.8. Metabolism of nucleotides	22
1.4. Metabolic modeling	22
1.4.1. Flux balance analysis	23
1.4.2. Metabolic flux analysis (MFA) and isotope balancing	23
1.5. Application of ¹³ C labeling in metabolic studies	25
1.5.1. ¹³ C Metabolic flux analysis	25
1.6. GFP fluorescence labeling	26
AIMS OF THE STUDY	27
MATERIALS AND METHODS	27
2.1. Yeast strains and cultivation media	27
2.2. Cultivation system and cultivation process routines	27
2.2.1. Cultivation system for the ¹³ C labeling experiments	28
2.2.2. Cultivation system for the stress response studies	28
2.3. Analytical methods	30
2.4. Calculation of absolute and conditional enrichments from ¹³ C NMR spectra	30
2.5. Calculation of theoretical absolute and conditional enrichments	33

RESULTS AND DISCUSSION	36
3.1 Metabolic network of <i>S. uvarum</i> determined by the ¹³ C labeling and metabolic modeling	36
3.1.1. Biosynthesis of amino acids of glutamate family	36
3.1.2. Biosynthesis of alanine	40
3.1.3. Biosynthesis of aspartate	41
3.1.4. Biosynthesis of trehalose	41
3.1.5. Reconstructed metabolic network of <i>Saccharomyces</i> spp. for the growth on glucose and acetate	43
3.2. Expression of LEA-like protein Hsp12p during the smooth change of stress conditions	45
CONCLUSIONS	47
REFERENCES	48
ACKNOWLEDGEMENTS	57
APPENDIX I	58
Mass balance equations of the intermediates of <i>S. cerevisiae</i> during the growth on mixed substrates of glucose and acetate	
Analytical solution of the linear equation system, consist of the independent metabolic fluxes of <i>S. cerevisiae</i> during the growth on mixed substrate of glucose and acetate	59
APPENDIX II	60
Yeast macromolecular composition, the concentration of individual monomers, and NADPH and NADH requirement for the biosynthesis	
PUBLICATIONS	61
KOKKUVÕTE	203
CURRICULUM VITAE	204
ELULUGU	205

INTRODUCTION

The importance of yeasts in biotechnology is enormous. A wide variety of yeast species are used in various food and beverage fermentation processes, however *S. cerevisiae* and *S. uvarum* are undoubtedly the most important species among them. In addition, a completely new area of yeast utilization has emerged in the pharmaceutical and medical areas, for example as a host organism for recombinant protein and vaccine production. Without decreasing the importance of *S. cerevisiae*, numerous other yeast species, e.g. *Kluyveromyces lactis*, *Hansenula polymorpha*, *Pichia pastoris*, *Schizosaccharomyces pombe* and *Yarrowia lipolytica* are gaining increasing attention for their potential use in modern fermentation biotechnology. Yeast is used as a model organism to study the peculiarities in the metabolic pathways of other eucaryotes as it shares many of the metabolic cycles and regulation mechanisms with a wide variety of eucaryotes.

The genome of *S. cerevisiae* was completely sequenced through a worldwide collaboration in 1997 (Goffeau, 1997). As a result, it is one of the best studied eucaryotic organisms and has been used in several creative and ambitious projects to explore the functions of gene products or gene expression on a genome-wide scale to provide a wide range of information about the genes, proteins and metabolic pathways. This information is now available in the genome databases such as *Comprehensive Yeast Genome Database* (Guldener et al., 2005), *Saccharomyces Genome Database* (Cherry et al., 1998), *Yeast Protein Database* (Hodges et al., 1998) and *Kyoto Encyclopedia of Genes and Genomes* (Kanehisa et al., 2004). While this genetic information is vast, it yields relatively limited insights about the cell as a system and about how it functions. This is due to the highly structured, complex, and interdependent interactions of genes and proteins which dynamically change in response to environmental factors. Thus, the individual function and collective interaction of genes, proteins and other cellular components in an organism as the response to the environmental conditions can be characterized together as an interaction network of cellular metabolism. This creates the need for models of the entire metabolic pathways that enable one to calculate the fluxes through individual intermediates towards the production of low molecular weight end products of the metabolism, such as proteinogenic amino acids or other cellular monomers. These kinds of models help us to understand the overall metabolic topology as a response to the environmental conditions.

There are some problems in applying only the genome databases for metabolic modeling: 1) different alternative pathways, 2) unknown localization of gene expression, and 3) unknown rates of enzymatic reactions. Other methods are used to obtain the data required for the elucidation of the functions and topology of metabolic networks under different environmental conditions. These include: mRNA arrays, determination of specific enzymatic activities or protein concentrations, and labeling experiments. The latter is especially efficient if combined with relevant cultivation methods. Analysis of labeling patterns allows one to not only distinguish between active and inactive pathways, but also quantify the fluxes through the different alternative pathways and determine their exact cellular localization.

In the present investigation two novel cultivation techniques for biomass labeling experiments were used: 1) D-stat for ^{13}C -labeling of biomass and 2) auxo-accelerostat for fluorescence labeling of small heat shock protein Hsp12p. The first was used in combination with metabolic modeling for more precise visualization of time-spatial structure of metabolic network, and the second for determination of yeast cell stress status as a response to different environmental conditions.

LITERATURE REVIEW

1.1. *Saccharomyces* spp.

The genus *Saccharomyces* (taxonomic classification: kingdom- fungi; phylum- *Ascomycota*; class- *Hemiascomycetes*; order- *Saccharomycetales*; family- *Saccharomycetaceae*; genus- *Saccharomyces*) was first described by Meyen and Hansen in 1883. It is yeast commonly isolated from human, mammals, birds, wine, beer, fruits, trees, plants, olives, and soil. The genus *Saccharomyces* includes several species, the most well-studied being *S. cerevisiae*. The other species in this genus are given in Table 1. *Saccharomyces* can be easily differentiated from other yeasts. Multipolar budding, production of ascospores, and fermentation profile aid in identification of *Saccharomyces* spp.

Table 1. Synonym and classification data for *Saccharomyces* spp. (all species accepted by Kurtzmann and Fell, 1997).

Species	Synonym
<i>Saccharomyces amurcae</i> (obsolete)	<i>Zygosaccharomyces fermentati</i>
<i>Saccharomyces anomalus</i> (obsolete)	<i>Pichia anomala</i>
<i>Saccharomyces bailii</i> (obsolete)	<i>Zygosaccharomyces bailii</i>
<i>Saccharomyces barnettii</i>	
<i>Saccharomyces bayanus</i>	
<i>Saccharomyces bisporus</i> (obsolete)	<i>Zygosaccharomyces bisporus</i>
<i>Saccharomyces carlsbergensis</i> (<i>Saccharomyces uvarum</i>)	
<i>Saccharomyces castelii</i>	
<i>Saccharomyces cidri</i> (obsolete)	<i>Zygosaccharomyces cidri</i>
<i>Saccharomyces dairenensis</i>	
<i>Saccharomyces delbrueckii</i> (obsolete)	<i>Torulaspora delbrueckii</i>
<i>Saccharomyces elegans</i>	<i>Saccharomyces aupagyucus</i>
<i>Saccharomyces exiguus</i>	
<i>Saccharomyces florentius</i>	<i>Zygosaccharomyces florentius</i>
<i>Saccharomyces glutinis</i>	<i>Rhodotorula mucilaginosa</i>
<i>Saccharomyces kluyveri</i>	
<i>Saccharomyces krusei</i>	<i>Candida krusei</i>
<i>Saccharomyces malacitensis</i>	<i>Zygosaccharomyces fermentati</i>
<i>Saccharomyces mellis</i>	<i>Zygosaccharomyces mellis</i>
<i>Saccharomyces microellipsoides</i>	<i>Zygosaccharomyces microellipsoides</i>
<i>Saccharomyces montanus</i>	<i>Zygosaccharomyces fermentati</i>
<i>Saccharomyces mrakii</i>	<i>Zygosaccharomyces mrakii</i>
<i>Saccharomyces neoformans</i>	<i>Cryptococcus neoformans</i>
<i>Saccharomyces nilssoni</i>	<i>Zygosaccharomyces fermentati</i>
<i>Saccharomyces paradoxus</i>	
<i>Saccharomyces pastorianus</i>	
<i>Saccharomyces rosinii</i>	
<i>Saccharomyces rouxii</i>	<i>Zygosaccharomyces rouxii</i>
<i>Saccharomyces ruber</i>	<i>Rhodotorula mucilaginosa</i>

1.2. *Saccharomyces uvarum*

Saccharomyces uvarum (alias *Saccharomyces carlsbergensis*), a bottom-fermenting (lager brewing) yeast is a species of yeast that belongs to genus *Saccharomyces* and was discovered in 1883 by Emil Christian Hansen. With further research by Martinus Willem Beijerinck in 1898, it was synonymized with *S. bayanus*. Until recently *S. bayanus* and *S. uvarum* were considered as conspecific because high DNA/DNA homology, but Nguyen and Gaillardin (2005) have suggested, based on the analysis of the coding sequences (CDS) of the *GDH1*, *MET2*, *HO*, *CDC91* and *BAP2*, that *S. bayanus* is a hybrid of *S. uvarum*/*S. cerevisiae* and thus can be reinstated as a distinct species, abolishing its previous status as synonym of *S. uvarum*.

Among the *Saccharomyces sensu stricto* strains defined by Vaughan-Martini and Kurtzman (1985) (contains three sibling species *S. cerevisiae*, *S. paradoxus*, *S. uvarum* and the hybrids between *S. cerevisiae* and *S. uvarum*, classified either as *S. bayanus* or as *S. pastorianus*), *S. uvarum* has been found to be the closest species to *S. cerevisiae* in terms of phylogeny (Bon et al., 2000; Kellis et al., 2003). Random sequence tags (RSTs) have allowed homologue identification up to 2789 open reading frames (ORFs) in both species (ORFs duplicate in *S. uvarum* but not in *S. cerevisiae*), centromeres, tRNAs, homologues of Ty1/2 and Ty4 retrotransposons, and a complete rDNA repeat. Only 13 RSTs in *S. uvarum* seem to be homologous to sequences in other organisms but not in *S. cerevisiae*. As the synteny between the two species is very high, cases in which synteny is lost suggest special mechanisms of genome evolution.

1.3. Metabolism and the metabolic network of *Saccharomyces* spp.

The main metabolic pathways (i.e. the biochemical assimilation and dissimilation of nutrients by the cell) for energy, biomass and product synthesis in *Saccharomyces* spp. are well defined (Fig. 1). The (relative) rate of individual reactions within the metabolic pathways depend on environmental conditions. The regulation of these pathways may take place at different levels:

1. enzyme synthesis, which comprises the induction, repression and derepression of the gene expression;
2. enzyme activity, which comprises allosteric activation, inhibition, or interconversion of the isoenzymes;
3. cellular compartmentalization, which comprises the localization of particular enzymes to the cytosol, mitochondria, peroxisomes, or vacuoles;
4. transport mechanisms, which comprise internalization, secretion and trafficking of the compounds between the cellular compartments and the external environment;
5. substrate and intermediate level, which determines the expression rates of genes of specific enzymes and reaction rates of enzymatic reactions.

Based on the metabolic pathways, the annotated genome sequence and experimentally determined biochemical and physiological characteristics for a given organism, the network of metabolic reactions can be reconstructed for the growth of cells under defined physiological and environmental conditions. An abundance of information about the individual genes, their expression products, compartmental localization and molecular functions (including the regulation, activities, and physical and genetic interactions) has been gathered into several genome databases. The information containing in these databases is organized into traditional pathways, such as glycolysis, pentose phosphate pathway, TCA cycle and pathways that lead to the synthesis of cellular monomers. The details are usually presented for the ORF name, gene name, enzyme name and EC number. Reconstruction of metabolic reaction networks in an organism begins with the thorough examination of the genome (Covert et al., 2001). Once the functional assignment of a sequenced genome is complete, the closest set of metabolic maps complementing the annotated genome should be outlined (Fig. 1), which can further be used as the templates for more precise reconstruction.

The reconstruction of metabolic networks in eucaryotic organisms also requires information about the compartmental localization of the individual metabolic reactions as well as the involvement of the transport steps across the cellular membranes. Förster et al. (2003) presented a first genome-scale *in silico* metabolic network for a eucaryotic cell on a basis of *S. cerevisiae* and compared the structure and metabolic capabilities of such a network with a genome-scale reconstructed metabolic network of *Escherichia coli*.

Despite the high-throughput technologies that enable the rapid generation of sequence, transcript, and proteomic data for any kind of organisms, we still cannot identify the number of metabolic genes that contribute significantly to the metabolic phenotype of an organism. This means, that decisions have to be made as to whether a reaction should be present in the reconstructed metabolic network or where is the exact compartmental localization of the given enzymatic reaction (Förster et al., 2003). A well-defined metabolic network itself is not sufficient for overall quantitative characterization of the behavior of the cell as a system. It is important to integrate the vast information from the genome databases into a reconstructed metabolic map which can be used for some qualitative predictions on the connectivities of the metabolites and other characteristics of network structure (Jeong et al., 2000). This allows for the selection of only the most relevant metabolic reactions which take place in the cell under specified physiological and environmental conditions. Once network reconstruction and metabolic maps have been developed and evaluated in the context of available biochemical and physiological information, they can be applied to various types of mathematical analysis (e.g. metabolic modeling).

1.3.1. Fermentative and respiratory metabolism of *Saccharomyces* spp.

It is well established that most yeasts, including *Saccharomyces* spp. employ sugars as their main carbon and energy source. The major source for energy production in *Saccharomyces* spp. is glucose and glycolysis is the general pathway for conversion of glucose to pyruvate, whereby the production of energy in form of ATP is coupled to the synthesis of intermediates and reduction power in form of NADH for biosynthesis. After glycolysis, two major modes of using pyruvate for further energy production can be distinguished: respiration and fermentation.

In the presence of oxygen and absence of glucose repression (i.e during the respiratory metabolism), pyruvate enters the mitochondrial matrix where it is oxidatively decarboxylated to acetyl-CoA by the pyruvate dehydrogenase multienzyme complex. This reaction also links the glycolysis to the TCA cycle in which the acetyl-CoA is completely oxidized to give two molecules of CO₂ and reductive equivalents in the form of NADH and FADH₂. The physiological transition state between the respiratory and fermentative metabolism is called the respiro-fermentative state (Käppeli et al., 1986; Fiechter and Seghezzi, 1992). During the respiro-fermentative growth the capacity of the enzymes of TCA cycle, especially pyruvate dehydrogenase becomes limited (Frick and Wittmann, 2005) due to excess glucose (or any other fermentative carbohydrate) flux into the mitochondria, and thus is a rate limiting step in a completely respiratory metabolism. The excess carbon entering the cytosolic pyruvate pool is thus directed towards pyruvate decarboxylase and fermentation. This phenomenon (simultaneous respiration and fermentation) is common for *Saccharomyces* spp. and is called the Crabtree effect (De Deken, 1966). The growth rate at which respiration becomes limited is called the critical growth rate (μ_{crit}). Further increase of the glycolytic flux and growth rate causes the on-set of the glucose repression (catabolic repression) and fermentative metabolism. This includes the decrease of flux through the TCA cycle, which results from direct repression of TCA cycle genes on the transcriptional level by the glucose repression system (Schüller, 2003) and the formation of glycerol in addition to ethanol, which is required to balance the NADH production during fermentative growth. The transitions between respiratory, respiro-fermentative and fermentative growth modes are illustrated in Figure 2.

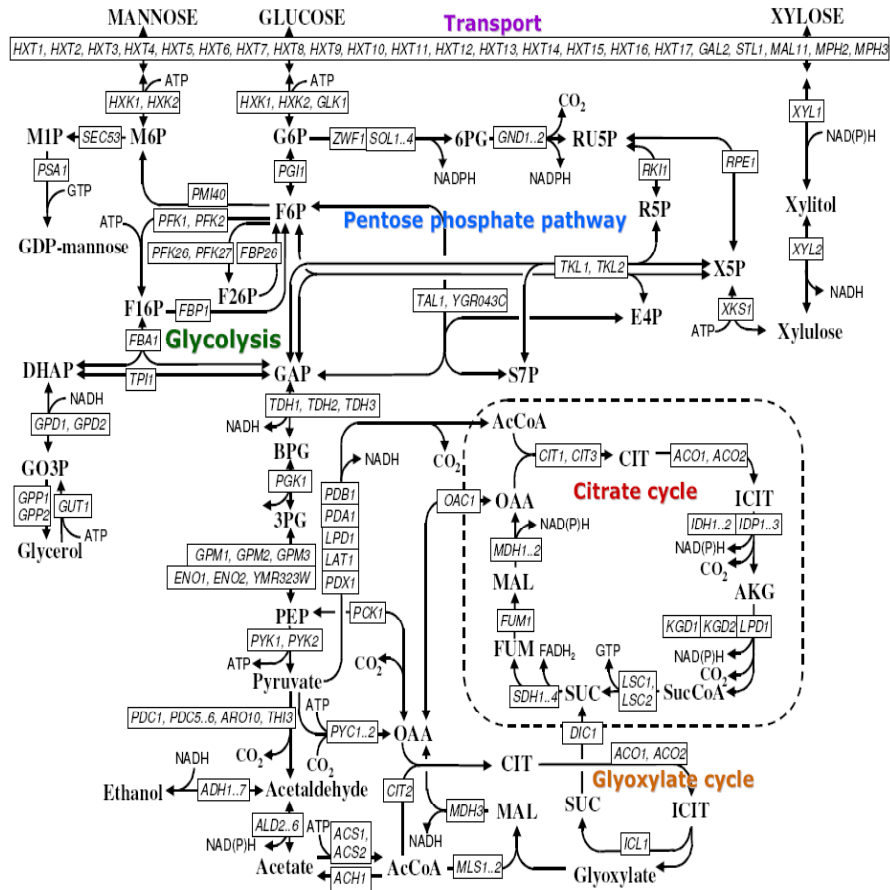


Fig. 1. Summary of the main metabolic networks in *S. cerevisiae* (Pitkänen, 2005). Gene names in the boxes are given according to the *Saccharomyces Genome Database*.

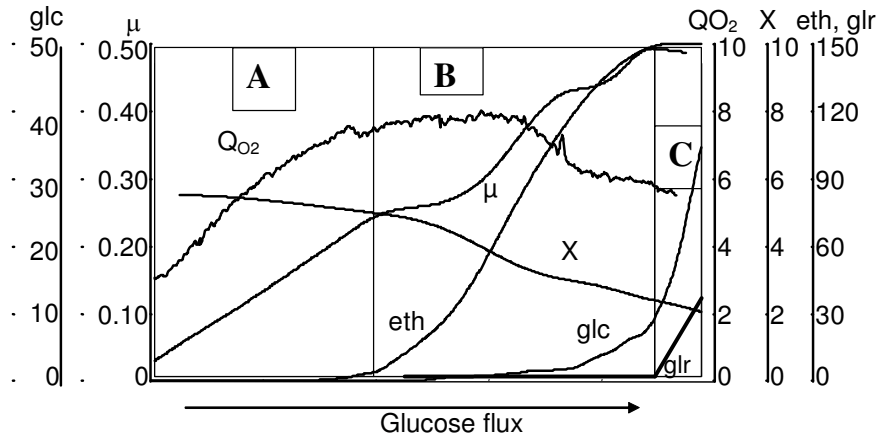


Fig. 2. Different growth modes of *Saccharomyces* spp. in aerobic conditions (Paper V): A – respiratory growth, (no ethanol and glycerol formation); B – respiro-fermentative growth (ethanol formation, no glycerol formation) and C – fermentative growth (ethanol and glycerol formation, respiration is repressed by glucose. glc, eth, glr – concentration of glucose, ethanol and glycerol in the cultivation media (g l⁻¹); μ - growth rate (h⁻¹); Q_{O2} – specific oxygen consumption rate by the cells (mol g⁻¹ h⁻¹); X – biomass concentration (g l⁻¹).

1.3.2. Glucose control mechanisms in *Saccharomyces* spp.

In *Saccharomyces* spp. the presence of glucose in the growth medium has dramatic effects on the physiology of the cells. As glucose is the most repressing sugar, the term "glucose repression" is often employed in terms of the control of gene expression (Fiechter et al., 1981; Käppeli, 1986). However, besides the regulation on a gene level (e.g. *FPS1*, *GAL1*, *GAL3*, *GAL4*, *GAL5*, *GLK1*, *HXK1*, *MEL1*, *FBP1*, *TPS1*, *TPS2*, *SUC2*) (Klein et al., 1998), glucose control also includes post-translational regulatory mechanisms: accelerated protein degradation e.g. carbon catabolite inactivation (or activation) of the target enzymes (e.g. inactivation of Mal2p, Mellp, Gal2p, Fbp1, Pck1p, Tps1p, Tps2p, Gsy2p or activation of Nth1p) (Holzer, 1976, Siro and Lövgren, 1978; DeJuan and Lagunas, 1986, Francois et al., 1991; Thevelein and Hohmann, 1995; Klein et al., 1998; Francois et al., 1991).

Glucose control requires glucose signaling. The two best investigated glucose signaling pathways are the main glucose repression pathway (Entian and Barnett, 1992; Gancedo, 1992; Trumbly, 1992, Klein et al., 1998) (Fig. 3) and the Ras-adenylate cyclase pathway (Thevelein, 1994; Thevelein et al., 2000) (Fig. 4). The main glucose repression pathway has the long-term function of keeping the cells repressed. The key elements in the main glucose repression pathway are the sensing hexokinase PII (Hxk2p), the serine/threonine protein kinase (Snf1p) and the DNA-binding repressor (Mig1p). It has been shown that Mig1p is increasingly phosphorylated with decreasing glucose concentration, and thus under the negative control of Snf1p (DeVit and Johnston, 1996). The Mig1p-controlled metabolic functions (i.e. the enzymes that have the putative Mig1p binding site) can be grouped into central metabolism (glycolysis, TCA cycle, fermentative and respirative functions, the glyoxylate shunt and gluconeogenesis), and the peripheral functions, such as the catabolism of sugars to the level of glucose-6-P (Klein et al., 1998). Another glucose control mechanism in yeast cells is related to the activity of cAMP-dependent protein kinases (cPKA) and PKA-related pathways (Thevelein et al., 2000). High PKA activity in yeast in the presence of glucose can be triggered by two pathways (Fig. 4). In the first one, the plasma membrane G-protein-coupled receptor Gpr1p interacts with the heterotrimeric G-protein alpha subunit Gpr2p and is responsible for the activation of adenylate cyclase Cyr1p and subsequent synthesis of cyclic AMP (cAMP). Additionally, the activity of Cyr1p is controlled at basal level by the Ras proteins (Ras1p and Ras2p) which belong to the family of G-proteins. The GDP/GTP ratio on Ras proteins is controlled by the guanine nucleotide exchange proteins (Cdc25p and Sdc25p) and by the GTP-ase activating proteins Ira1p and Ira2p. The cAMP signal triggers a cPKA-mediated protein phosphorylation cascade, carried out by the three catalytic subunits (Tpk1p, Tpk2p and Tpk3p) which phosphorylate the target proteins (such as the enzymes of trehalose and glycogen metabolism, stress resistance, cell wall lyticase resistance and expression of a variety of genes controlled by *STRE*-elements in their promoter). However, this effect is only transient when only glucose is added or if one of the other essential substrates is missing from the growth medium. The second pathway of PKA-related glucose control in yeast is involved in maintaining the PKA-mediated effects and is called the fermentable growth medium induced pathway (FGM) (Thevelein, 1994). The FGM-pathway requires glucose and a complete growth medium to sustain the PKA-dependent phosphorylation (Fig. 4). Activation of the FGM pathway does not require cAMP but requires catalytic activity of cPKA subunits and Sch9p which is a protein kinase that is homologous to the catalytic subunits of cPKA encoded by *TPK* genes. Although cAMP is not involved as a second messenger, the FGM pathway maintains a phenotype consistent with high PKA activity during growth on glucose. The exact sensing system for glucose and other essential nutrients for activation of FGM pathway remain to be elucidated.

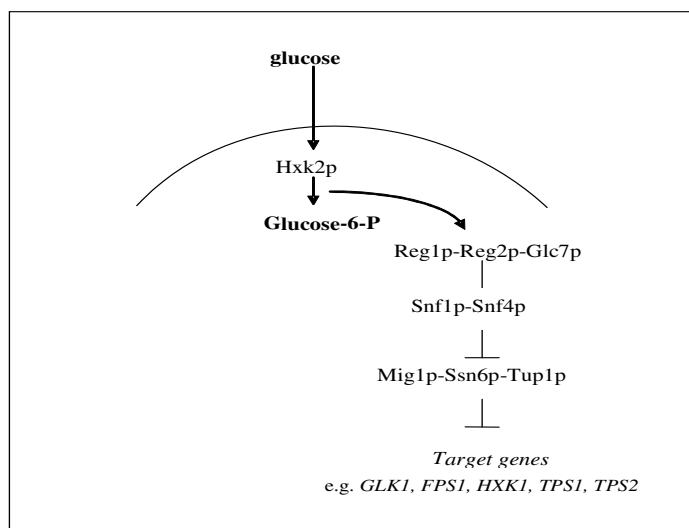


Fig. 3. Scheme of the main glucose repression pathway in *S. cerevisiae* (Klein et al., 1998). The sensing hexokinase Hxk2p phosphorylates rapidly fermentable sugars and also exhibits protein kinase activity by phosphorylating the phosphatase 1 complex (Glc7p, Reg1p and Reg2p) which dephosphorylate part of the protein kinase complex (Snf1p and Snf4p). The Snf1p and Snf4p are activated by phosphorylation in derepressing conditions and inactivated by dephosphorylation in repressing conditions. The DNA-binding Mig1p is a protein which enters the nucleus when dephosphorylated, and directs the actual repressors Ssn6p and Tup1p to the putative binding sites of the repressed genes.

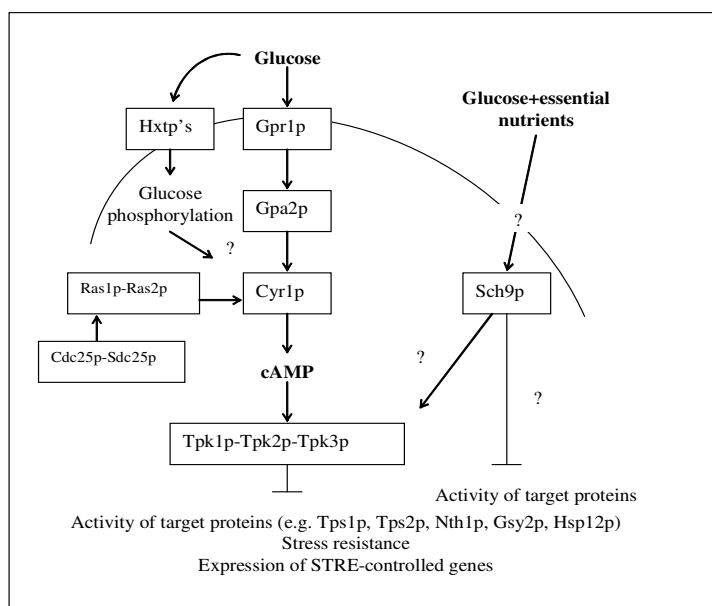


Fig. 4. Scheme of glucose control mechanisms based on cAMP-dependent protein kinases (cPKA) and the fermentable growth medium (FGM) pathway (Thevelein et al., 2000).

1.3.3. Stress response in *Saccharomyces* spp. and heat shock proteins

All living cells display a rapid cellular response, usually called a stress response to adverse environmental conditions. Such stressful environmental conditions are, for example, high temperature, high osmolarity, oxidative stress, nutrient starvation etc. Common response of the cells to these stresses is the synthesis of a set of stress-response proteins, so called heat shock proteins (HSPs) (Craig et al., 1994).

Several HSP families can be distinguished according to their molecular weight in *Saccharomyces* spp.: high molecular weight Hsp104p and Hsp83p, and low molecular weight

Hsp30p, Hsp26p and Hsp12p. In addition, several other proteins, such as some glycolytic enzymes, ubiquitin and plasma membrane proteins are synthesized in addition to the regular HSPs upon the exposure of the cells to stressful conditions and thus can also be called heat shock proteins (Mager and De Kruijff, 1995). Yeast Hsp104p cannot be detected during normal growth on fermentable carbon sources. In contrast, the expression is strongly induced upon the exposure of the cells to heat shock (Sanchez and Lindquist, 1990) as well as when the cells enter the stationary phase. It has been demonstrated that Hsp104p acts as a protein disaggregation mediator during heat shock (Parsell et al., 1994). Hsp83p belongs to the family of Hsp90p and is encoded by two different genes *HSP83* and *HSC83* (heat shock cognate). While the expression of *HSC83* is only weakly induced upon stress exposure, *HSP83* transcription is strongly activated upon heat shock (Mager and De Kruijff, 1995). The first of the yeast low molecular weight family heat shock proteins, Hsp30p is localized in the plasma membrane under stress conditions (Piper et al., 1994) and has been proposed to serve as a regulator of the plasma membrane ATPase Pma1p (Weitzel et al., 1987). The other two small HSPs in yeast, Hsp26p and Hsp12p or late embryogenesis abundant (LEA) protein represent a diverse group of HSPs. A universal property of these proteins is their developmental regulation, however, their complete functions are still to be elucidated.

Hsp12p has been shown to protect cell membranes against desiccation and ethanol-induced stress, due to its plasma membrane location (Sales et al., 2000). The induction of synthesis of HSP12p increases remarkably during the heat shock as well as on entry into stationary phase and when cells are subjected to osmostress and higher ethanol concentration in the growth media (Motshwene et al., 2004; Karreman and Lindsey, 2005; Paper VII). The *HSP12* gene is activated by the high-osmolarity-glycerol MAP kinase pathway (Fig. 5) and has been reported to be under negative control by cAMP (Fig. 4) (Mager and Ferreira, 1993; Varela et al., 1995, van Wuytswinkel et al., 2000).

1.3.4. High-osmolarity-glycerol pathway in *Saccharomyces* spp.

The high-osmolarity-glycerol (HOG) MAP kinase pathway is an important signal transduction pathway in yeast and mediates the cellular response to the higher external osmolarity conditions. Two transmembrane osmosensors Sho1p and Sln1p participate in HOG mitogen-activated protein kinase (MAPK) cascade by different mechanisms (Siderius et al., 1997; van Wuytswinkel et al., 2000) (Fig. 5). A putative osmosensing receptor Sho1p triggers a MAPK kinase (MAPKK) Pbs2p activity through the stimulation of MAPK kinase kinase (MAPKKK) and activates the MAPK Hog1p. Another osmosensing mechanism involves a histidine kinase osmosensor Sln1p and a phosphorelay intermediates Ypd1p and Ssk1p. The Ypd1p binds to both Sln1p and Ssk1p and mediates the multistep phosphotransfer reaction (phosphorelay). The consecutive phosphorylations of MAPKKK (consist of two homologues Ssk22p and Ssk2p) and MAPKK Pbs2 result in activation of Hog1p. Although the exact molecular targets of Hog1p in the nucleus has not been yet clarified, it was shown to be involved in different processes, such as increased gene transcription (e.g. *HSP12*, *CTT1*, *GPD1*) and glycerol levels during the hyperosmotic shock (Rep et al, 1999).

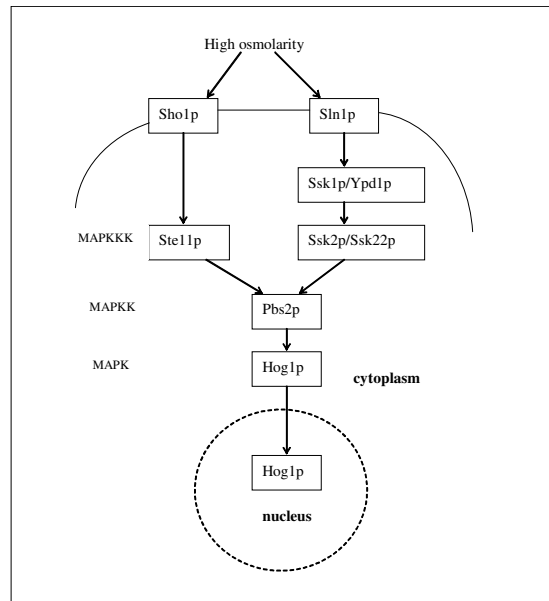


Fig. 5. Scheme of the HOG pathway in *S. cerevisiae* (Van Wuytswinkel et al., 2000).

1.3.5. Amino acid metabolism

With regard to nitrogen metabolism, most yeasts belonging to *Saccharomyces* spp. are capable of assimilating wide range of inorganic and organic nitrogen sources to biosynthesize amino acids and proteins. They possess a whole repertoire of genes capable to synthesize all amino acids and thus the simple inorganic nitrogen sources such as ammonia can be used as the sole nitrogen source. A scheme of the metabolic pathways and metabolic precursors involved in amino acid biosynthesis in *S. cerevisiae* is given in Figure 6.

1.3.5.1. Biosynthesis of the amino acids of glutamate family

Biosynthesis of glutamate

Ammonium utilization in *Saccharomyces* spp. occurs exclusively via its incorporation into glutamate and glutamine (Magasanik, 1992), a process that can be achieved by two distinct metabolic routes: 1) the concerted action by enzymes glutamine synthetase (Gln1p) and NADH-dependent glutamate synthase (Glt1p) (Roon et al., 1974); and 2) pathway catalyzed by the two isoenzymes of NADP-dependent glutamate dehydrogenase (Gdh1p and Gdh3p) which catalyses the reductive amination of α -ketoglutarate to form glutamate (Holzer and Schneider, 1957; Benachenhou-Lahfa et al., 1993). While *GLT1* and *GDH3* are expressed in the mitochondria, *GDH1* and *GLN1* are expressed in the cytosol (DeLuna et al., 2001; Kumar et al., 2002; Sickmann et al., 2003; Magasanik 2003). Which one of those two pathways is functional *in vivo* depends probably on the growth conditions.

Biosynthesis of proline and arginine

Proline and arginine are both synthesized from glutamate. The first five steps of arginine biosynthesis in *S. cerevisiae* take place in the mitochondria through a row of consecutive reactions catalysed by acetylglutamate synthase (Arg2p), acetylglutamate kinase and N-acetyl-gamma-glutamylphosphate reductase (Arg5p, Arg6p), acetylornithine aminotransferase (Arg8p) and acetylornithine acetyltransferase (Arg7p) (Hinnebusch, 1992; Abadjieva et al., 2001) which result in the formation of ornithine. Ornithine is further exported from the mitochondria to the cytoplasm (Crabeel et al., 1996) where the conversion to L-arginine is carried out via the three reactions mediated by ornithine carbamoyltransferase (Arg3p), arginosuccinate synthase (Arg1p) and argininosuccinate lyase (Arg4p). Proline is synthesized

from glutamate in the cytosol via the intermediates γ -glutamyl phosphate, γ -glutamyl semialdehyde and Δ -pyrroline-5-carboxylic acid (P5C). The three enzymes involved in this pathway are γ -glutamyl kinase (Pro1p), γ -glutamyl phosphate reductase (Pro2p) and P5C reductase (Pro3p) (Li and Brandriss, 1992).

1.3.5.2. Biosynthesis of the amino acids of pyruvate family

Biosynthesis of alanine

Pyruvate is the precursor for alanine biosynthesis, which can take place by the activities of two putative alanine transaminases (mitochondrial Alt1p and cytosolic Alt2p). It is important to note that the exact biological process and the regulation mechanisms of alanine synthesis are still unknown. Also, there has been some controversy about the exact compartmental localization of alanine biosynthesis in *S. cerevisiae* (Maaheimo et al., 2001; dos Santos et al., 2003). The exact localization of the reaction depends probably on the growth conditions.

Biosynthesis of valine and leucine

Plants, bacteria and fungi (including *Saccharomyces* spp.) can synthesize valine and leucine via a common pathway (Duggleby and Pang, 2000). Condensation of two molecules of pyruvate to 2-acetolactate catalyzed by the two subunits of mitochondrial acetolactate synthase (Ilv2p, Ilv6p) serve as the first step of synthesis (Ryan et al., 1973, Ryan and Kohlhaw, 1974). Further conversion reactions to valine and leucine are catalyzed by the set of enzymes: acetohydroxyacid reductoisomerase (Ilv5p), dihydroxyacid dehydratase (Ilv3p) and two branched-chain amino acid transaminases (Bat2p and Bat1p) for valine, and α -isopropylmalate synthase two isozymes (Leu9p and Leu4p), isopropylmalate isomerase (Leu1p), β -isopropylmalate dehydrogenase (Leu2p), and Bat2p and Bat1p for leucine respectively. Biosynthetic reactions of valine and leucine biosynthesis in *Saccharomyces* spp. are localized in the mitochondria.

1.3.5.3. Biosynthesis of the amino acids of aspartate family

Biosynthesis of aspartate and asparagine

Biosynthesis of aspartate is a result of the consecutive reactions catalyzed by two highly similar pyruvate carboxylase isozymes (Pyc1p, Pyc2p), which convert pyruvate to oxaloacetate, and following the transfer of the amino group from glutamate to oxaloacetate by aspartate aminotransferase, consist of the two isozymes (Aat1p and Aat2p). The isozyme encoded by *AAT1* represents the mitochondrial location (Morin et al., 1992) while *AAT2* codes for the cytosolic and peroxisomal aspartate aminotransferase activities and has been reported to be active in glucose-grown cells (Verleur et al., 1997; Michal, 1998; Maaheimo et al., 2001). Synthesis of aspartate during the respiratory growth on glucose has been shown to be localized in the cytosol (Maaheimo et al., 2001). Synthesis of asparagine from aspartate is catalyzed by the two cytosolic isozymes (Asn1p, Asn2p).

Biosynthesis of threonine

In *Saccharomyces* spp. threonine formation from homoserine (derived from aspartate) is catalyzed in two steps: phosphorylation of homoserine by homoserine kinase (Thr1p) at the expense of ATP to render *O*-phosphohomoserine and subsequent elimination of orthophosphate by threonine synthase (Thr4p) to yield threonine. While the subcellular localization of homoserine kinase is unknown, threonine kinase is expressed in the cytosol (Huh et al., 2003).

Biosynthesis of isoleucine

For the biosynthesis of isoleucine, mitochondrial acetolactate synthase (two subunits Ilv6p, Ilv2p) catalyses the condensation of pyruvate and 2-oxobutyrate, which arises from threonine, to 2-aceto-2-hydroxybutyrate and further proceeds with conversion to isoleucine catalyzed by the same enzymatic reactions as for valine synthesis (Ilv5p, Ilv3p, Bat2p and Bat1p respectively).

Biosynthesis of methionine

Yeasts belonging to *Saccharomyces* spp. can directly assimilate inorganic sulfur for the biosynthesis of sulfur-containing amino acids (Masselot and De Robichon-Szulmajster, 1975). Such a direct sulfhydrylation pathway for the biosynthesis of methionine involves the biosynthesis of homoserine from aspartate, which is also a precursor in threonine biosynthesis. The first step here is a phosphorylation of aspartate by the cytosolic aspartate kinase (aspartate-4-P transferase) (Hom3p) to yield aspartyl-4-P which is further converted into homoserine via a row of consecutive reactions carried out by NADPH-dependent aspartic semialdehyde dehydrogenase (Hom2p) and homoserine dehydrogenase (Hom6p). Homoserine is then activated through esterification to form the *O*-acetyl homoserine by homoserine-*O*-acetyltransferase (Met2p). Hydrogen sulfide (H₂S), the final product of microbial sulfate reduction reacts with *O*-acylated homoserine, with replacement of the acetyl group by sulfide to form homocysteine, a reaction catalyzed by *O*-acetyl-homoserine thiol-lyase (Met17p). Homocysteine is then methylated to methionine via a cobalamin-independent enzyme methionine synthase (Met6p).

1.3.5.4. Biosynthesis of lysine

In *Saccharomyces* spp. lysine is synthesized via the L-alpha-aminoadipic pathway from α -ketoglutarate and acetyl-CoA by the consecutive enzymatic reactions catalyzed by homocitrate synthase (Lys20p, Lys21p), homoaconitase (Lys4p), alpha aminoadipate reductase (Lys2p) and saccharopine dehydrogenase (Lys9p, Lys1p) (Zabriskie and Jackson, 2000). Indirect evidence that the enzymes of the α -aminoadipate synthesis are located in the mitochondria has been provided (Betterton et al., 1968), however, recently the nuclear subcellular localization of the two isoforms of homocitrate synthase was demonstrated (Chen et al., 1997).

1.3.5.5. Biosynthesis of the amino acids of 3-phosphoglycerate family (the serine-glycine-cysteine group)

Biosynthesis of serine and glycine

Glycine and serine biosynthesis may proceed via different alternative pathways in *Saccharomyces* spp. (Albers et al., 2003): 1) the “threonine pathway” where glycine is formed via cytosolic threonine aldolase (Gly1p) and subsequent formation of serine from glycine and 5,10- methylene-tetrahydrofolate (THF) by mitochondrially located serine hydroxymethyltransferases (Shm1p, Shm2p) (Sinclair and Dawes, 1995); 2) the “glyoxylate pathway” in which glyoxylate from anaplerotic glyoxylate cycle is converted to glycine by the activity of mitochondrial alanine:glyoxylate transaminase (Agx1p) (Schlosser et al., 2004) and then further to serine by serine hydroxymethyltransferases (Shm1p, Shm2p). The latter can be functional only during the growth on non-fermentable carbon sources since both the formation of glyoxylate and Agx1p needed for this biosynthetic pathway are glucose-repressed (Melcher and Entian, 1992). 3) The “phosphoglycerate pathway” is the third alternative for serine and glycine biosynthesis, in which the first reaction is catalyzed by two cytosolic isozymes of phosphoglycerate dehydrogenase (Ser3p, Ser33p), producing 3-phosphohydroxypyruvate plus NADH from the glycolytic intermediate 3-phosphoglycerate and NAD⁺. The enzymes of the subsequent two reactions are cytosolic phosphoserine transaminase (Ser1p) and phosphoserine phosphatase (Ser2p) which convert 3-phosphohydroxypyruvate over 3-phosphoserine to serine.

Biosynthesis of cysteine

Biosynthesis of cysteine starts from serine which is combined through a condensation with homocysteine (synthesized through the same reactions from aspartate as in case of methionine) to form cystathione. The reaction is catalysed by cystathione beta-synthase (Cys4p). Cystathione is then cleaved at the γ position by cystathione gamma-lyase (Cys3p) to produce cysteine (Ono et al., 1988).

1.3.5.6. Biosynthesis of aromatic amino acids

The reactions catalyzed by the eight enzymes (Aro3p, Aro4p, Aro1Cp, Aro1Ep, Aro1Dp, Aro1Bp, Aro1Ap, Aro2p) of the shikimate pathway in cytosol from erythrose 4-P (E4P) and phosphoenolpyruvate (PEP) to chorismic acid are common for the synthesis of all aromatic amino acids (phenylalanine, tyrosine and tryptophane) in *Saccharomyces* spp. (Braus, 1991). Chorismic acid is the last common intermediate for the three amino acids and distributed towards phenylalanine-tyrosine and tryptophan branches. In the phenylalanine-tyrosine branch chorismate is converted to prephenate (Aro7p), which is the last common intermediate before the pathway branches again toward either phenylalanine or tyrosine. The two enzymatic reactions are involved into phenylalanine synthesis from prephenate over phenylpyruvate (Pha2p, Aro8/9p) and into tyrosine over 4-hydroxyphenyl-pyruvate (Tyr1p, Aro8/9p). The tryptophan branch proceeds in five steps from chorismate to tryptophane using the six enzyme activities (Trp2/3Cp, Trp4p, Trp1p, Trp3Bp, Trp5) encoded by five genes.

1.3.5.7. Biosynthesis of histidine

The precursor that serves for histidine biosynthesis is ribulose-5-phosphate (R5P) which is converted to 5-phospho-ribosyl-pyrophosphate (PRPP) by its synthetase (Prs4p). The following six-step conversion of PRPP into imidazole glycerol phosphate (IGP) and 5'-phosphoribosyl-4-carboxamide-5-aminoimidazole (AICAR) (His1p, His4p, His6p, His7p) requires glutamine as the source of the amide nitrogen. AICAR is recycled into the *de novo* purine biosynthetic pathway. The other product, IGP, is dehydrated by one of the activities of the bifunctional enzyme (His3p). The resulting enol is ketonized nonenzymatically to imidazole-acetol-phosphate (IAP). The next step of the pathway consists of a reversible transamination involving IAP and a nitrogen atom from glutamate which leads to the production of α -ketoglutarate and L-histidinol-phosphate (HOL-P) (His5p). The latter is then converted to L-histidinol (HOL) (His2p). During the last two steps of histidine biosynthesis, HOL is oxidized to the corresponding amino acid L-histidine, catalyzed by the enzyme histidinol dehydrogenase (His4p).

trehalose-P phosphatase (Tps2p) (Bell et al., 1998) (Fig. 7). Both components of the trehalose synthase/phosphatase complex have been reported to be subject to glucose repression and catabolite inactivation (Thevelein and Hohmann, 1995). Trehalose hydrolysis in *Saccharomyces* spp. is carried out by the enzymes cytosolic neutral trehalase (Nth1p) and acid trehalase (Ath1p). The latter has a vacuolar localization. A third enzyme, encoded by *NTH2*, is 77% identical to Nth1p, but does not appear to be involved in trehalose catabolism, since its null mutant exhibits normal levels of neutral trehalase activity (Nwaka et al., 1995). The activities of trehalose synthase complex and neutral trehalase are antagonistically controlled by cAMP-dependent phosphorylation by protein kinase A (cPKA) (Fig.4).

As in the case of many other high molecular mass biopolymers, the synthesis of glycogen involves three steps: initiation, elongation and ramification (Francois and Parrou, 2001). Glycogen synthesis in the cytosol of *Saccharomyces* spp. is initiated by enzyme glycogenin with its two isozymes (Glg1p, Glg2p) (Fig. 7). This produces a short α -(1,4)-glycosyl chain that is further elongated by glycogen synthase (two isozymes Gsy1p and Gsy2p). The synthesized chains are ramified by the branching enzyme (Glc3p) which transfers a block of 6-8 residues from the end of a linear chain to an internal glucosyl unit and thus creates α -(1,6)-linkage. Degradation of glycogen in *Saccharomyces* spp. can occur via two pathways: 1) amylolysis catalysed by α -[1,4] and α -(1,6)-glucosidases that produce glucose (Clancy et al., 1982) which is common in sporulating cells; and 2) by sequential reactions involving phosphoryloysis (Gph1p) and debranching activities (Gdb1) which produce glucose-1-P and glucose (Francois and Parrou, 2001) (Fig. 7). As in the case of trehalose synthesis and degradation, glycogen synthase is under the ultimate control of protein kinases (cAMP dependent PKA and Snf1p) (Sunnarborg et al., 2001). Additionally, dephosphorylation has been shown to act as the main deactivation mechanism of glycogen synthase. Biochemical data indicate that this phosphorylation-dephosphorylation “equilibrium” is antagonistically controlled by the levels of glucose-6-P and cAMP. However, the exact mechanism by which high levels of cAMP favor glycogen synthase phosphorylation is not clarified (Francois and Parrou, 2001).

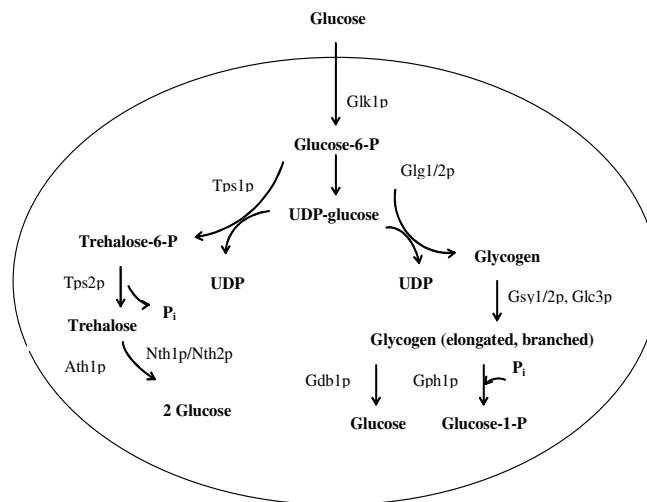


Fig. 7. The metabolic pathways of glycogen and trehalose synthesis and degradation in *Saccharomyces* spp. (François and Parrou, 2001).

1.3.7. Metabolism of lipids

Synthesis of lipids in *Saccharomyces* spp. is similar to that in other organisms, starting from glycerolphosphate and fatty acids in cytosol. The input to fatty acid synthesis in yeast cytosol is acetyl-CoA which is carboxylated to malonyl-CoA (Hasslacher et al., 1993; Kohlwein et al., 1996). The acetyl-CoA and malonyl-CoA bind to the complex, and become ester linked to serine hydroxyl group before being transferred into a thioester linkage with the phosphopantetheine thiol. The condensation reaction involves decarboxylation of the malonyl moiety and the following transfer of the carboxyl group to the chain. When the fatty acid is 16-carbon atoms long, a thioesterase domain catalyzes hydrolysis of the thioester, linking the fatty acid to phosphopantetheine. The 16-carbons long saturated fatty acid palmitate is the final product of the fatty acid synthase complex. Elongation beyond the 16 carbon palmitate occurs in mitochondria and endoplasmic reticulum (ER). Polyunsaturated fatty acids esterified to coenzyme A are substrates for the ER elongation machinery, which uses malonyl-CoA as donor of 2-carbon units.

1.3.8. Metabolism of nucleotides

Purine and pyrimidine nucleotides are major energy carriers, subunits of the nucleic and ribonucleic acids (DNA, RNA) and precursors for the synthesis of nucleic cofactors, such as NAD. The *de novo* pathway leading to the purine (AMP and GMP) synthesis starts by phosphorylation of ribose-5-P to phosphoribosyl pyrophosphate (PRPP), carried out by the enzyme PRPP synthetase (encoded by *PRS* genes), followed by nine consecutive reactions (enzymes encoded by *ADE*-genes) leading to the synthesis of inosine 5-monophosphate (IMP) (Hartman and Buchanan, 1959). The presence of L-aspartate and glutamine are necessary to form the IMP structure. Conversion of IMP to AMP over adenylosuccinate (by cytosolic Ade12p, Ade13p) and GMP over xanthosine 5'-P (by cytosolic Imd1p and Gua1p) is further carried out to complete the synthesis of purine nucleotides. After the first phosphorylation by adenylate kinase (Adk1p, Adk2p) or guanylate kinase (Guk1p) and reduction by ribonucleotide reductases (Rnr1p, Rnr2p, Rnr3p and Rnr4p), followed by the second phosphorylation by nucleoside diphosphate kinase (Ynk1p) of both AMP and GMP, dATP and dGTP are formed respectively. The first two steps in pyrimidine nucleotide synthesis is catalysed by aspartate transcarbamylase (Ura2p) which catalyses the reaction from L-glutamine to carbamoyl-P and further to carbamoyl-L-aspartate in a reaction with L-aspartate. The next six reactions lead to the synthesis of uridine-3-P (UTP) (catalyzed by Ura4p, Ura1p, Ura5p, Ura10p, Ura3p and Ura6p). Cytidine-5'-triphosphate (CTP) is formed by an amination of UTP, catalyzed by CTP synthase two isozymes (Ura7p, Ura8p).

1.4 Metabolic modeling

Information derived from the reconstructed metabolic networks is not sufficient to completely specify the metabolic phenotypes of an organism that will be expressed under given environmental conditions (Edwards et al., 2002). As the metabolic phenotypes can be defined in terms of flux distributions through a metabolic network, interpretation and prediction of the metabolic flux distributions should be carried out by means of mathematical modeling and computer simulation.

Quantitative metabolic modeling of a single cell as a system has been the subject of 20 years of research. Domach and co-workers launched a visionary project around 1980 (Domach et al., 1984; Domach and Schuler, 1984). Their goal was to construct a computer simulation of the growth of *E. coli*, based on the basic processes of substrate uptake rates, catabolic reactions, production of precursor metabolites of the final metabolites, synthesis of macromolecules, and cell envelope and cell volume accumulation. The construction of metabolic models is necessary for understanding and manipulating effectively the complex biological systems such as cell is. A hierarchy of methods for utilizing information on metabolism has been proposed by Bailey (1998). This hierarchy develops from external in- and outfluxes (such as substrate consumption and product excretion rates), and boundaries within a cell such as a particular metabolic network in a whole cell or particular organelle, defined by a modeller. A common method of relating cell genotype to cell phenotype is the

analysis of the fluxes in the metabolic network (Covert et al., 2001). Several approaches of cellular flux-based analysis have been proposed: 1) pathway analysis; 2) flux-balance analysis (FBA) and 3) metabolic flux analysis (MFA). While the pathway analysis is a method for generally defining the structure of the metabolic network as it relates to the overall metabolic capabilities of the organism using current information of genomics and proteomics (Schilling and Palsson, 2000), the FBA and MFA are used to predict the metabolic fluxes and their quantitative values by means of only mathematical models (FBA), or in combination with the experimental data (MFA).

1.4.1. Flux balance analysis (FBA)

Flux balance analysis can be used to calculate, interpret and predict metabolic flux distributions and to analyze the capabilities of a metabolic network based on the reaction stoichiometry of the system as well as the thermodynamic and reaction capacity constraints (Edwards et al., 2002).

The basic principle of how FBA is performed is shown in Figure 8. After the reconstruction of metabolic network (A), the dynamics of integrated metabolic networks are described in the form of dynamic mass balances (B). It is assumed that the system operates under steady state conditions, i.e. the concentration of each metabolite considered in the system will remain constant over time. In other words, the sum of fluxes into an intermediate has to equal the sum of fluxes leaving the intermediate (C). Once the system has been defined in terms of these mass balance constraints, the additional constraint equations based on the measurement of external fluxes, labeling pattern and knowledge of the system are added (D). Thus, the system of fluxes can be calculated from a few well chosen measured fluxes, which effectively defines the capabilities of the system. If the number of fluxes (unknowns) is higher than the number of equations (metabolites) it will be impossible to solve the equations algebraically, however, optimization can be used with regards to the desired parameter in order to calculate the internal fluxes (E). Usually this is done by quantitative maximization of the necessary fluxes in order to maximize the biomass yield or product excretion. The final step in flux balance analysis is the system analysis (F) where the analysis of the system behavior is carried out under different conditions (e.g. by varying the constraints and adding or removing metabolic reactions within the system).

1.4.2. Metabolic flux analysis (MFA) and isotope balancing

Compared to FBA, MFA measures the flux distribution in more detail, by estimating the internal fluxes based on a combination of isotope labeling and balancing techniques, followed by mathematical analysis (Christensen and Nielsen, 2000¹; Tran-Dinh et al., 1996, Christensen et al., 2002, Cannizzarro et al., 2004). The FBA technique alone does not provide complete information on the distribution of the intracellular fluxes in the system, even if the external fluxes are measured. Especially in the case where uncertainties in the flux pattern exist (Fig. 9). Metabolic labeling and isotope balancing is widely used to overcome these shortcomings and gather more information to complement flux models (Paalme et al., 1982¹; Paalme et al., 1982²; Walker et al., 1982; Chance et al., 1983; Tran-Dinh et al., 1996; Szyperski et al., 1996; Christensen and Nielsen, 2000²; Christensen et al., 2002; Cannizzarro et al., 2004).

Isotope balancing can be carried out either on atom-level or molecular-level. The atom-level (fractional enrichment) isotope balance is similar to the metabolite balance where the sum of labeled carbon atoms entering a given position of a metabolite has to equal the sum of labeled carbon atoms leaving from the same position. Thus, the only difference between metabolite balancing and atom-level isotope balancing is that the fluxes in and out of a carbon position in a metabolite are weighted with respect to the fractional enrichments of the carbon atoms involved. In order to describe the carbon transitions in a row of metabolic reactions to express the isotope balances so-called atom-mapping matrices can be used (Zupke and Stephanopoulos, 1994; Christensen and Nielsen, 2000²) (Fig. 10).

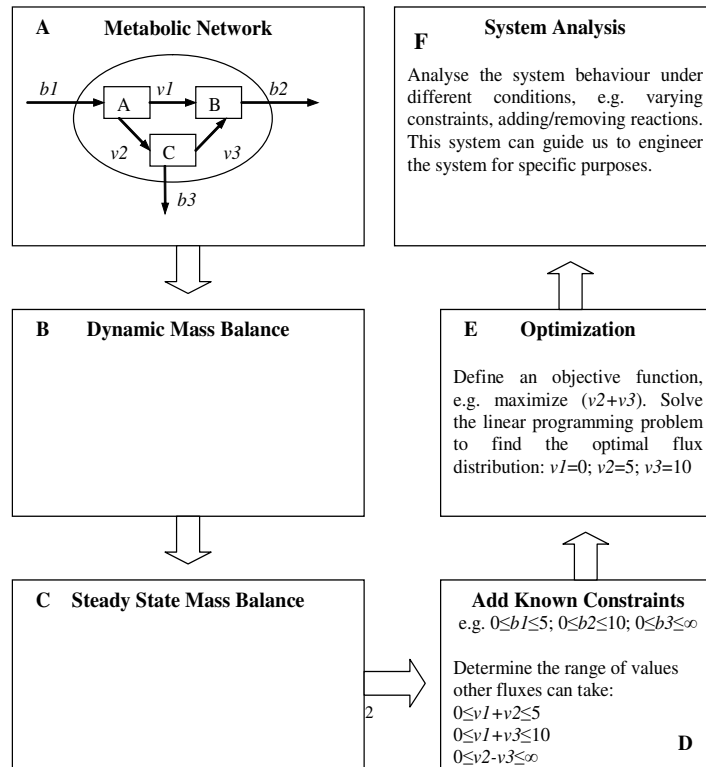


Fig. 8. The basic principle of FBA (Edwards et al., 2002).

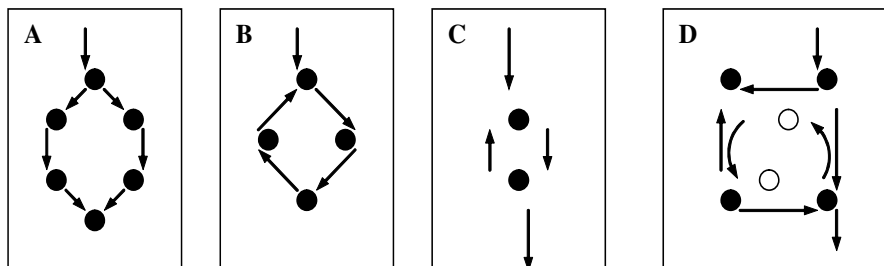


Fig 9. Typical situations in which stoichiometric MFA fails (Wiechert, 2001): A – parallel pathways without any related flux measurements; B – metabolic cycles; C – bidirectional reaction steps; and D – split pathways when cofactors are not balanced.

Contrary to atom-level isotope balancing, where the enrichments of the certain fraction of carbons is considered, isotope balancing on a molecular-level is based on a certain combination of labeled carbon atoms. Considering that only ^{12}C and ^{13}C isotopes are present in the carbon backbone of a molecule M with n carbon atoms, the total combination of 2^n labeling states can be calculated (Fig. 11) (Malloy et al., 1988). The percentage of the molecules in any specific labeling state is referred to as the isotopomer fraction. Determination of isotopomer distribution and calculation of the corresponding isotopomer fractions provides the most detailed description about the distribution of metabolic fluxes. However, it still has its own limitations. For example, carrying out the isotopomer labeling experiments only makes sense if powerful methods for measuring isotopomer fractions are available (Wiechert et al., 1999). In addition, the complexities may arise when the bimolecular reactions are involved in the system, as the positional isotopomer generated by such reactions is a function of the positional isotopomer distribution in both of the precursor molecules. Due to this, the use of positional isotopomers is primarily limited to the unimolecular reaction containing systems such as TCA cycle (Christensen and Nielsen, 2000¹).

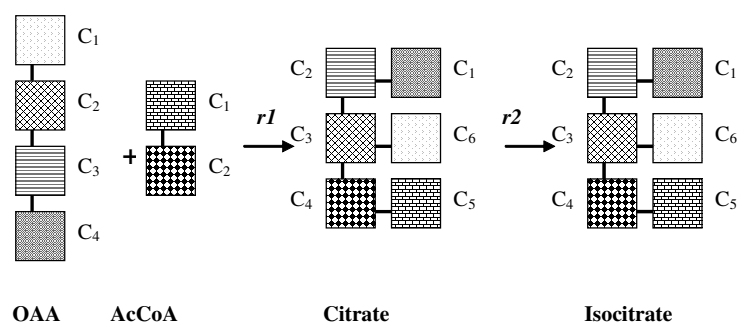


Fig. 10. Example of carbon atom-mapping matrices in condensation reaction of acetyl-CoA and oxaloacetate to citrate and following isomerization of citrate into isocitrate. Carbon atoms at different positions are marked with different patterns (Zupke and Stephanopoulos, 1994).

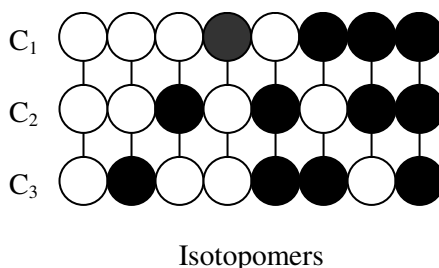


Fig 11. The positional isotopomers of a three-carbon molecule with total 8 possible labeling states.

1.5. Application of ^{13}C labeling in metabolic studies

The most often used isotope in metabolic analysis is magnetically active ^{13}C . This method is the direct successor of that with radioactive ^{14}C which was used to establish the pathway identification and flux quantification experiments since the end of 1940s (Blum and Stein, 1982). The main advantage in using ^{13}C compared to ^{14}C is that it is far more stable and easy to determine using nuclear magnetic resonance (NMR) or gas chromatography-mass spectrometry (GC-MS). Also safety considerations usually impose a practical upper limit to the concentration of ^{14}C that may be used experimentally. Besides ^{13}C , other magnetically active isotopes which are less naturally abundant, such as ^{15}N and deuterium are used in the labeling experiments for more specific purposes (Vanatalu et al., 1993; Lafaye et al., 2005; Tomson et al., 2006). However, using ^{13}C allows one to gain the most comprehensive and detailed information for describing and quantifying the overall metabolic network in the cells.

1.5.1. ^{13}C Metabolic flux analysis

^{13}C MFA is based on carbon-labeling experiments where the specifically ^{13}C -labeled substrate (e.g., ^{13}C -[1]-glucose or ^{13}C -uniformly labeled glucose) is used in the cultivation media either as a sole carbon source or in a mixture with non-labeled substrates (Dos Santos et al., 2003). Once the substrate is catabolized in the cell, the labeled carbon atoms are distributed all over the metabolic network and the ^{13}C enrichments in the intracellular metabolite pools can be measured using either GC-MS or ^{13}C -NMR. The resulting data in the form of absolute or conditional enrichments (Paalme et al., 1982^{1,2}; Paper VI) provide a large amount of additional information for the identification of the active pathways and quantification of metabolic fluxes (if the isotope balancing and the computational methods are applied). In addition, one can narrow down the compartmental localization of the specific reactions of the

metabolic network. The latter is especially important if the metabolism of eucaryotic organisms is under study.

Measurements of labeling patterns of intracellular intermediates are difficult to perform due to the small pool sizes, their low stability, and difficulties in separation. However, because amino acids, as the final metabolic products, are present in relatively large quantities and are stable, their ^{13}C enrichments can be used to reflect the labeling patterns and enrichments of various important central intermediates (Paalme et al., 1982^{1,2}, Christensen and Nielsen, 2000; Maaheimo et al., 2001).

1.6. GFP fluorescence labeling

The cloning and expression of green fluorescence protein (GFP) (Prasher et al., 1992), a highly fluorescent protein from the luminescent jellyfish *Aequorea victoria*, has attracted wide interest in the fluorescence labeling of cells, subcellular organelles and biomolecules. Traditionally, fluorescence labeling was accomplished through purification of the protein and then subsequently covalently conjugating them to reactive derivatives of organic fluorophores. The stoichiometry and location of the dye attachment is often difficult to control and careful purification of the proteins is usually necessary. Moreover, if the proteins are to be used *in vivo*, a final step to get them across the plasma membrane is required, which is a rather complicated process. An alternative is to use molecular biological means to generate fluorescent proteins. In this work we use a technique which is widely used and practical. It involves the concatenation of the gene for nonfluorescent protein of interest with a gene of naturally fluorescent protein, such as GFP, thus expressing the fusion protein (Chalfie et al., 1994; Rizzuto et al., 1995; Straight et al., 1996; Mateus and Avery, 2000). Recent advances in electronic light microscopy together with the application of GFP and other *in vivo* staining techniques have allowed novel and exciting insights into structural organization and dynamics of cells as small as yeast. Numerous methods for protein tagging with GFP have been described (Ross-Macdonald et al., 1997; Kohlwein, 2000). The increased application of GFP as well as yellow fluorescent protein (YFP) as a tag for microscopic analysis in living yeast cells for subcellular localization studies has provided a wealth of localization data in the literature. So far, the most comprehensive localizome established using chromosomically tagged GFP is for a collection of *S. cerevisiae* strains, covering two thirds of the proteome (Huh et al., 2003). Matsuyama et al. (2006) used YFP tagging of the ORFs to determine the localization of 4431 proteins in *Schizosaccharomyces pombe*, corresponding to ~90 % of the fission yeast proteome.

Besides the localizome studies, fluorescence labeling is also increasingly used in defining the metabolic responses to different environmental factors. For example, it has been demonstrated that the expression of heat shock protein Hsp12p and Gfp2p fusion protein construct in brewer's yeast is a rapid method to determine the stress status of the cells under different environmental conditions known to induce *HSP12* transcription (salt, osmotic, ethanol and heat stress). In addition, fluorescence labeling was used to determine the exact localization of Hsp12p (Karreman and Lindsey, 2005; Paper VII).

AIMS OF THE STUDY

The aims of the present study were as follows:

1. comprehend the metabolic network of *S. uvarum*, based on the results of ^{13}C labeling experiments using ^{13}C labeled Na-acetate and unlabeled glucose, including the reconstruction of the metabolic network under specified cultivation conditions through the use of metabolic modeling;
2. to demonstrate the efficiency ^{13}C labeled Na-acetate as a relatively low-cost substrate for metabolic labeling experiments;
3. to study the effect of smoothly changing stress conditions on the expression of Hsp12p in *S. cerevisiae* using the fluorescent molecular label Hsp12p-Gfp2p fusion protein.

MATERIALS AND METHODS

2.1. Yeast strains and cultivation media

Commercially produced bottom-fermenting brewer's yeast strain *S. uvarum* W34 was used in the ^{13}C -labeling studies, and was kindly provided by Dr. Richard Degré (Lallemand, Inc., Canada). A defined dilution media (Paalme et al., 1997) containing unlabeled glucose (2.6 and 2.8 g l⁻¹ respectively) and labeled [1,2]- ^{13}C (99 %) or [2]- ^{13}C Na-acetate (90 %) (1.06 or 0.76 g l⁻¹ respectively) was used for the labeling of biomass.

The Hsp12p-Gfp2p construct of *S. cerevisiae* for stress response studies under smoothly changing environmental conditions was kindly provided by Prof. George Lindsey (University of Cape Town, South Africa). Complete synthetic dropout medium without uracil was used, containing: glucose, 20 g l⁻¹; NaCl, 1 g l⁻¹; CaCl₂, 1 g l⁻¹; KH₂PO₄, 6 g l⁻¹; (NH₄)₂SO₄, 5 g l⁻¹; MgSO₄, 1 g l⁻¹; FeSO₄*7H₂O, 5 mg l⁻¹, MnSO₄*5H₂O, 1.6 mg l⁻¹; ZnSO₄*7H₂O, 1.6 mg l⁻¹; CoCl₂*5H₂O, 0.3 mg l⁻¹; CuCl₂*5H₂O, 0.3 mg l⁻¹; Na₂MoO₄*H₂O, 0.3 mg l⁻¹; adenine, 10 mg l⁻¹; L-histidine, 20 mg l⁻¹; L-leucine, 100 mg l⁻¹; L-tryptophan, 50 mg l⁻¹; and vitamins (added separately through the 20 µm filter into the sterilized medium): myo-inositol, 20 mg l⁻¹; thiamine, 4.4 mg l⁻¹; pyridoxine, 1.2 mg l⁻¹; Ca-pantothenate, 0.5 mg l⁻¹; d-biotin, 0.03 mg l⁻¹. The pH of the medium was adjusted to 4.5 using 5 M H₂SO₄. The same medium was used for the inoculum and auxo-accelerostat cultures. The shift-up experiments with NaCl (100, 400 and 800 mM) and temperature (35 and 37 °C) were carried out in culture withdrawn from the fermenter during the turbidostat cultivation after the steady state had been obtained (OD₆₀₀=1.0 or 2.0 depending on the experiment).

2.2. Cultivation system and cultivation process routines

A common strategy for metabolic studies of microorganisms is to keep the environmental conditions as constant as possible. The main problem in using the batch cultivations for these experiments is the low number of cell generations which can be obtained during the constant (maximum) growth rate. At the same time, the change of the environmental conditions (pH, biomass concentration, substrate and product concentrations etc.) during the biomass growth result in rather complicated interpretation of the experiment results. In a fed-batch culture, it is possible to keep the physiological conditions of the growing cells close to steady-state. The process can be carried out for extended periods at constant specific growth rates and substrate consumption rates (Paalme et al., 1990). However, in this case the steady-state conditions can be obtained only when the biomass concentration has become too high, which can further have an unpredictable effect on the behavior of the cell physiology. In this work, the modifications of the continuous cultivation methods D-stat (Paper II; Paper III) and auxo-accelerostat (Adamberg et al. 2003; Paper VIII) were used for the labeling experiments and stress response studies.

2.2.1. Cultivation system for the ^{13}C labeling experiments

The chemostat cultivation with changing culture volume (Dunn and Mor, 1975) was used for the ^{13}C labeling experiments. This combination of fed-batch and continuous chemostat culture, where all the parameters except the culture volume are kept constant, allowed us to obtain quasi-steady-state and collect a sufficient amount of culture sample for analysis (Paper IV; Paper VI) (Fig. 12).

The cultivation system consist of a custom vessel with a working volume of 250 ml, an ADI 1030 biocontroller with an AD/DA interface connected to a PC using the cultivation control program “BioXpert” (Applikon, The Netherlands), and a commercial version of the laboratory software “FermXpert” (Vinter *et al.*, 1992) was used. The fermenter was equipped with pO_2 , pH and temperature sensors, and balance to measure the weight of the outflow of the cultivation media for precise dilution rate calculation in chemostat mode. A variable speed pump and a fixed speed pump were used for the dilution media and culture outflow respectively (using the overflow tube). The pH was kept at 4.5 by titration with 1 N HCl. Two different dilution rates ($D=0.04$ and 0.08 h^{-1}) were used in separate experiments.

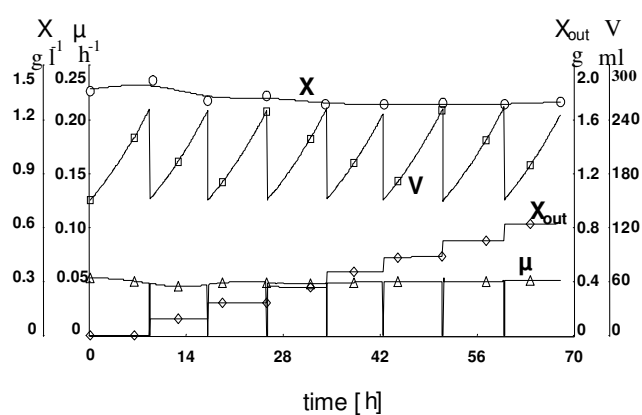


Fig. 12. The D-stat cultivation of *Saccharomyces uvarum* W34 at constant dilution rate ($D=0.04\text{ h}^{-1}$) with changing culture volume (Paper IV). X – biomass concentration (g l^{-1}); μ – specific growth rate (h^{-1}); X_{out} – total amount of biomass taken out from the fermentor (g); V – culture volume (ml).

Cultivation was started in chemostat mode ($V=150\text{ ml}$) with a dilution media containing unlabeled glucose and acetate. Chemostat cultivation was carried out for at least 5 culture volumes to obtain steady state conditions, and then the dilution media was switched to the one containing the labeled Na-acetate and the outflow pump was stopped. The pumping rate of the dilution media was increased according to the increasing cultivation volume to maintain a constant dilution rate. When the cultivation volume reached 250 ml, 100 ml of culture was pumped out within 1 min into the collection tube on ice and the cultivation was continued at a volume of 150 ml again. The process was repeated 12 times in order to get a sufficient amount of labeled biomass for NMR analysis. After the labeled biomass was collected, the procedure was repeated using nonlabeled substrates for quantification of the cell biomass components.

2.2.2. Cultivation system for the stress response studies

The auxo-accelerostat, a turbidostat-based cultivation method with smooth change of one of the environmental parameters, was used for stress response studies (Paper VII). The cultivation system consisted of a 500 ml Biobundel fermenter (Applikon, The Netherlands) with a working volume of 250 ml, an ADI 1030 biocontroller, and AD/DA interface connected to a PC with the cultivation control program “BioXpert” (Applikon, The Netherlands), and a commercial version of the laboratory software “FermXpert”. The fermenter was equipped with pO_2 , pH and temperature sensors, an optical density detector (Optek, Germany) and balances to measure the weight of the fermenter and feeding media for

precise dilution rate calculation. The cultivation medium in the fermenter (250 ml) was inoculated with 15 ml of inoculum grown overnight in a shake flask and then cultivated in batch mode at pH=4.5 and T=30°C until the desired cell density OD₆₀₀=1.0 or 2.0 was reached. At this point the feeding with fresh cultivation media was started. The feeding rate was feed-back controlled to the OD set-point at 20 second intervals. The variable speed pumps were used to control the optical density of the culture. The culture volume was kept constant by controlling the weight of the fermenter using the outflow pump. A fixed speed pump was used for titration with 1 N NH₄OH to control the cultivation pH. After steady state conditions were reached in turbidostat (characterized by a constant specific growth rate), the smooth change of cultivation temperature (rate of change 1 °C h⁻¹) or NaCl concentration (rate of change 30 mM NaCl h⁻¹) in the fermenter was started. In the experiments with the smooth increase of NaCl, an additional pump for cultivation media with high NaCl concentration (1 mol l⁻¹) was used. In the experiments with the smooth increase of cultivation temperature, the temperature was increased according to the preset profile. The dilution rate was calculated using the following equations:

$$D = \frac{pmp_{in}}{V} \quad (1)$$

$$pmp_{in} = \frac{-d(balance_2 + balance_3)}{dt} + pmp_{alk} \quad (2)$$

$$V = \frac{balance_2}{\rho} \quad (3)$$

where D – dilution rate, pmp_{in} – total flow rate of the feeding into the fermenter, balance₂ – weight of the main cultivation media, balance₃ – weight of the NaCl containing cultivation media, pmp_{alk} – alkali titration rate, V – volume of the culture medium in the fermenter, ρ – specific gravity of the cultivation media.

The optical density, glycerol and ethanol concentrations, as well as the fluorescence magnitude were plotted against time and extrapolated using the “BioXpert” spline option to calculate the growth and stress response characteristics. On the basis of the curves obtained, the specific growth rate (μ , h⁻¹), ethanol and glycerol production rate (Q_{eth} ; Q_{glr} , mmol g dwt⁻¹ h⁻¹), the specific Hsp12p synthesis rate (HSP_s , U OD⁻¹ h⁻¹), and the ratio of glycerol to ethanol formation (Y_{GE} , mol mol⁻¹) were calculated using the following equations:

$$\mu = D + \frac{d(OD)}{dt \cdot OD} \quad (4)$$

$$Q_{eth} = \frac{eth \cdot (pmp_{out})}{V \cdot OD \cdot \gamma} + \frac{d(eth)}{dt * OD \cdot \gamma} \quad (5)$$

$$Q_{glr} = \frac{glr \cdot (pmp_{out})}{V \cdot OD \cdot \gamma} + \frac{d(glr)}{dt * OD \cdot \gamma} \quad (6)$$

$$HSP_s = \frac{dF}{dt} + \mu * F \quad (\text{auxo-accelerostat}) \quad (7)$$

$$HSP_s = \frac{dF}{dt} \quad (\text{shift-up experiments in batch culture}) \quad (8)$$

$$Y_{GE} = \frac{Q_{glr}}{Q_{eth}} \quad (9)$$

where V - current fermenter volume, pmp_{out} - outflow rate of the culture broth from the fermenter, OD - optical density at 600 nm, γ - biomass conversion constant ($\gamma = dwt/OD_{600}$), eth - ethanol concentration in the culture, glr - glycerol concentration in the culture, F - specific fluorescence of the cells (in arbitrary units).

2.3. Analytical methods

The concentration of EtOH, glucose, acetate and glycerol were determined using a “Waters” HPLC equipped with UV and refractive index detectors. Separation of the metabolites was achieved by isocratic elution (0.6 ml min^{-1}) using a BioRad HPX-87H column (BioRad Laboratories Inc., USA) with $0.009 \text{ N H}_2\text{SO}_4$. Concentration of NaCl in the culture was calculated based on the Na^+ and Cl^- concentrations determined in the supernatant using ion chromatography. An anion column IC-Pak A (lithium borate/gluconate eluent), a cation column IC-Pak C (EDTA/nitric acid eluent), and a “Waters 432” conductivity detector were used for the analysis. The ^{13}C NMR spectra of proteinogenic amino acids and trehalose were obtained on a Bruker AMX500 pulsed Fourier transform spectrometer operating at 125.7 MHz under conditions of complete proton composite pulse (waltz16) decoupling using internal deuterium field lock. Free induction decays were accumulated as 64 K data points with Fourier transformations in 256 K. The bandwidth of 30 kHz and about 30 degree 2 (μs) observation pulses with relaxation delay of 1 s were used. “Mestre-C” software was used to process the spectra. Expression of *HSP12* was quantified by measuring the fluorescence intensity of Hsp12p-Gfp2p fusion protein using a Fluo-Imager M53 system (Skalar, The Netherlands) by scanning at an excitation wavelength from 400 to 520 nm and an emission wavelength from 420 to 615 nm. The biomass components were determined as described in Paper VI.

2.4. Calculation of absolute and conditional enrichments from ^{13}C -NMR spectra

When substrate containing the ^{13}C label is fed to the cells the labeled carbons become distributed in the whole active metabolic network and are accumulated in the final products of metabolism such as the monomers that make up the macromolecular composition of the cells. In the labeled molecules two different types of fractional carbon enrichment, so called absolute and conditional enrichment can be calculated for every carbon position in the respective molecule. In a ^{13}C NMR spectrum the isotopomer distribution is well resolved because a labeled carbon atom produces different hyperfine splitting signals depending on the labeling state and magnitude of its direct neighbors in the molecule, as described in Figure 13. If the neighboring carbon atoms are not labeled, only a single peak (singlet) is observed. If one of the neighboring carbons is labeled, the coupling of the two labeled carbons into a doublet is observed in addition to the singlet peak. The size of the doublet splitting (usually referred as a coupling constant) depends on the molecule under study and the functional group in which the labeled neighbor is situated. A third possibility is that both of the neighboring carbons are labeled. In this case the splitting of the doublets into doublets (a quartet) can be observed if the resolution is sufficient. However, when both doublet splittings are equal (coupling constants are equal) no resolution is possible and only a triplet can be observed. Completely unlabeled carbon produces no NMR signal.

In a proton decoupled ^{13}C NMR spectra the resulting peak multiplet intensities (corresponding to the each carbon atom in a molecule) are proportional to the number of labeled carbon atoms in the sample. The absolute enrichment of a molecule refers to the ratio of the number of labeled carbons to the total number of carbons in a molecule and was calculated using equation:

$$E = \frac{{}^{13}\text{C}}{{}^{12}\text{C} + {}^{13}\text{C}} \quad (10)$$

Internal standards and quantification of the concentration of the compound in both the sample and calibration sample was necessary to calculate the precise absolute ${}^{13}\text{C}$ enrichments from NMR spectra. The calculation of the absolute ${}^{13}\text{C}$ enrichments was carried out as follows:

$$E_j = \frac{E_{st} * M_j * C_{st}}{M_{st} * C} * \frac{M_{st}' * C'}{M_j' * C_{st}'} \quad (11)$$

where E_{st} - ${}^{13}\text{C}$ enrichment of the internal standard in the sample, M_j - total intensity of the peaks corresponding to the j^{th} carbon in the sample, C_{st} - concentration of the internal standard in the sample, M_{st} - total intensity of the standard reference peak(s) in the sample, C - concentration of the compound under study, M_{st}' - total intensity of the standard reference peak in the calibration sample, C' - concentration of the compound in the calibration sample, M_j' - total intensity of the peaks corresponding to the j^{th} carbon in the calibration sample and C_{st}' - concentration of the reference compound in the calibration sample. The peak intensity was referred to as the integrated value of the peak surface, or the height of the peak in the multiplet under study.

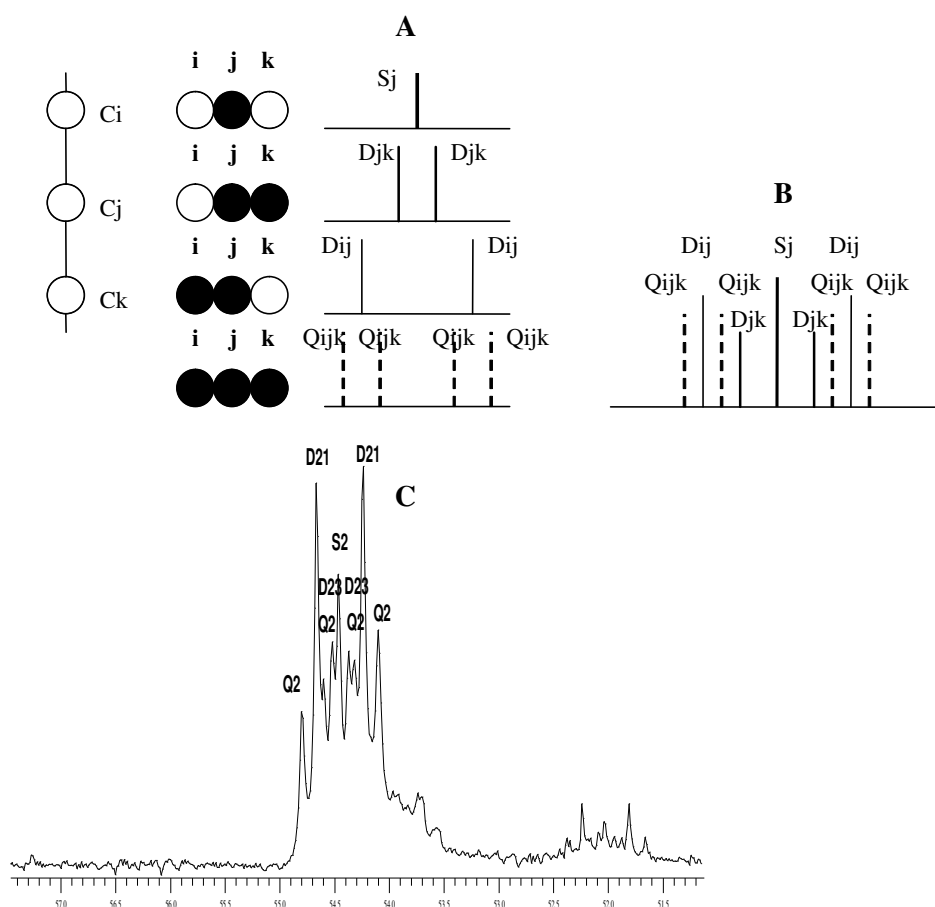
In parallel with the calculation of absolute enrichments, an approach described in Paalme et al. (1982¹) was also used to determine the so called conditional ${}^{13}\text{C}$ enrichments, which represent the enrichment of a certain carbon position in the molecules where the neighboring carbon(s) are also labeled (eq.12). The calculation of the conditional enrichments from the ${}^{13}\text{C}$ NMR spectra is possible because of the splitting of the carbon lines due coupling with the neighboring carbons and, in contrast to the calculation of absolute enrichments, it does not require any additional analytical procedures and thus makes it relatively easy to perform. In addition, due to the different labeling combinations arising from the isotopomer distribution, the determination of conditional enrichments is much more informative compared to the absolute enrichments. The conditional enrichments were calculated as follows:

$$E_i^j = \frac{D_{ij} + Q_j}{D_{ij} + Q_j + S_j + D_{jk}} \quad (12)$$

where E_i^j - enrichment of i^{th} carbon in those molecules where j^{th} carbon is also labeled, D_{ij} - total intensity of the doublet belonging to the adjacent j^{th} carbon arising due to the ${}^{13}\text{C}$ - ${}^{13}\text{C}$ coupling between the j^{th} and i^{th} carbon, Q_j - total amplitude of the quartet belonging to the adjacent j^{th} carbon arising due to the ${}^{13}\text{C}$ - ${}^{13}\text{C}$ coupling between the j^{th} carbon, i^{th} carbon and k^{th} carbon, S_j - total amplitude of the singlet of j^{th} carbon, and D_{jk} - total amplitude of the doublet belonging to the adjacent j^{th} carbon arising due to the ${}^{13}\text{C}$ - ${}^{13}\text{C}$ coupling between the j^{th} carbon and k^{th} carbon.

For example, the conditional enrichment of C_0 in those molecules where C_α was also enriched, was calculated based on the eq. 12 and the ${}^{13}\text{C}$ NMR spectra of glutamate from the labeling experiment with ${}^{13}\text{C}$ -[1,2] Na-acetate (Figure 13). Calculation of ${}^{13}\text{C}$ conditional enrichments in the molecules where only two adjacent carbons were labeled was carried out using the following equation:

$$E_i^j = \frac{D_{ij}}{D_{ij} + S_j} \quad (13)$$



Multiplet	Height of the corresponding multiplet (in arbitrary units)
Singlet S_{α} (S_2)	2.230
Doublet $D_{\alpha\beta}$ (D_{23})	$2 * 1.208$
Doublet $D_{\alpha 0}$ (D_{21})	$2 * 3.025$
Quartet $Q_{0\alpha\beta}$ (Q_{123})	4.1425

$$E_1^2 = \frac{D_{21} + Q_2}{D_{21} + Q_2 + S_2 + D_{23}} * 100\% = \frac{2 * 3.025 + 4 * 1.425}{2 * 3.025 + 4 * 1.425 + 2.23 + 2 * 1.208} * 100\% = 72\%$$

Fig 13. Typical ^{13}C NMR spectra evolving from a metabolite with three adjacent carbon atoms: separate lines arising from coupling with respective neighboring labeled atom(s) (A), the whole NMR spectra (multiplet) with different peak intensities if all three adjacent carbons in a molecule are labeled (B). The middle carbon atom produces a singlet, two kinds of doublet, or doublet doublet (quartet) depending on the labeling state of its neighbours. An example is given below for a glutamate C_2 (C_{α}) position and for calculation of conditional enrichment E_1^2 (E_0^{α}) as determined in the present investigation (C) (Paper VI).

2.5. Calculation of theoretical absolute and conditional enrichments

Calculation of metabolic fluxes from the stoichiometric model of S. cerevisiae

In order to compose the stoichiometric model based on the metabolic network of *S. cerevisiae* and calculate the metabolic flux values, several assumptions were made:

1. concentrations of all the intermediates in different compartments of the cell (i.e. cytosol and mitochondria) are constant over time;
2. chemical composition of the cell is constant (i.e. the concentration of any of the compound consist in the biomass does not change over time);
3. consumption rates of substrates and product excretion rates are constant over time;
4. metabolic network is identical in all cells of the culture.

Hence, the model did not calculate the changes of the cell composition and flux values which may occur due to the cell cycle. The initial metabolic network for the growth of the cells on mixed substrate of glucose and acetate was composed based on the literature data (Maaheimo et al., 2001) and *Saccharomyces Genome Database*. Metabolic fluxes were quantified using the linear equation system obtained from the flux balances through the individual intermediates and assuming that the sum of the fluxes into the intermediate is equal to the sum out of the intermediate (eq. 14). To simplify the equation system and have the equal number of equations and fluxes, only the most important and energetically optimal fluxes were considered.

$$fluxes_{IN} - fluxes_{OUT} = \frac{dS_i}{dt} \quad \left(\frac{dS_i}{dt}\right) = 0 \quad (14)$$

The other important fluxes in the system, such as the substrate consumption rates and production rates of the biomass components were given according to their experimentally measured values. In addition to the stoichiometric balance equations for intermediates, similar equations were also written for the NADH and NADPH balances in both the cytosol and mitochondria. Hence, considering that the fluxes in and out of the intermediate can be expressed as specific rates ($\text{mmol g}^{-1} \text{biomass h}^{-1}$) and the concentration of intermediate remains constant in time span (eq. 14), the mass balance equations were written for every individual intermediate resulting in a linear equation system for the entire metabolic network. A total of 34 metabolites (equations) were involved in the linear equation system (Appendix 1). As the number of fluxes was 38 (degree of freedom = 4) the values for the following fluxes were taken as: *GLK1* – determined from the experiments (specific consumption rate of glucose - q_{GLC}); *ACS2* – determined from the experiments (specific consumption rate of acetate - q_{ACE}); *X* – const. (intercompartmental exchange flux of α -ketoglutarate was 0); *MAE1*- variable. Values for the consumption of key intermediates (o_i) for cellular biosynthesis were calculated based on the macromolecular composition of biomass determined from the experiments, and based on their monomer composition (either determined experimentally or taken from Cortassa et al., 1995):

1. $o_1(\text{G6P}): C_{\text{glycogen}} + C_{\text{glucan}} + C_{\text{trehalose}}$
2. $o_2(\text{F6P}): C_{\text{mannan}} + C_{\text{peptidoglycans}}$
3. $o_3(\text{R5P}): C_{\text{histidine}} + C_{\text{dAMP}} + C_{\text{dGMP}} + C_{\text{dCMP}} + C_{\text{dUMP}}$
4. $o_4(\text{E4P}): C_{\text{phenylalanine}} + C_{\text{tryptophane}} + C_{\text{tyrosine}}$
5. $o_5(\text{G3P}): C_{\text{glycerol-P}}$
6. $o_6(\text{3PG}): C_{\text{cysteine}} + C_{\text{glycine}} + C_{\text{serine}} + C_{\text{dAMP}} + C_{\text{dGMP}}$
7. $o_7(\text{PEP}): 2C_{\text{phenylalanine}} + C_{\text{tryptophane}} + 2C_{\text{tyrosine}}$
8. $o_{8m}(\text{PyT}_m): C_{\text{alanine}} + 2C_{\text{isoleucine}} + 2C_{\text{leucine}} + 2C_{\text{valine}}$
9. $o_{8c}(\text{PyT}_c): C_{\text{alanine}}$

10. $o_{9c}(\text{AceCoA}_c)$: $C_{\text{lysine}} + 5C_{\text{lauric acid}} + 7C_{\text{palmitoleic acid}} + 8C_{\text{oleic acid}}$
11. $o_{9m}(\text{AceCoA}_m)$: C_{leucine}
12. $o_{10c}(\text{Oxa}_c)$: $C_{\text{asparagine}} + C_{\text{aspartate}} + C_{\text{methionine}} + C_{\text{threonine}} + C_{\text{dUMP}} + C_{\text{dCMP}}$
13. $o_{10m}(\text{Oxa}_m)$: $C_{\text{isoleucine}} + C_{\text{aspartate}}$
14. $o_{11c}(2\text{kg}_c)$: $C_{\text{glutamine}} + C_{\text{lysine}} + C_{\text{proline}}$
15. $o_{11m}(2\text{kg}_m)$: $C_{\text{arginine}} + C_{\text{glutamate}}$
16. $o_{12}(\text{SucCoA})$: heme compounds

Calculation of theoretical absolute enrichments

According to the reconstructed metabolic network the simplified scheme of ^{13}C label movement from ^{13}C -[1,2] acetate into the main intermediates of TCA cycle was composed (Fig. 14). Based on the origin of the carbon fragments of proteinogenic amino acids (atom mapping matrices) from the single intermediates, the exact theoretical labeling pattern was derived and the probabilities of ^{13}C labeling for every carbon position in the proteinogenic amino acids were calculated as follows:

$$p_i = \frac{p_A^i * flux_A + p_B^i * flux_B}{flux_A + flux_B} \quad (15)$$

where p_i - probability of ^{13}C labeling of position i in the compound under study, p_A^i and p_B^i - probabilities of ^{13}C labeling of corresponding positions in the precursor molecules A and B, and $flux_A, flux_B$ - corresponding fluxes from the precursor molecules.

Calculation of theoretical conditional enrichments

Theoretical absolute enrichments (i.e the ^{13}C enrichment in one-carbon fragments) of the metabolic intermediates are equal to the probabilities of labeling of the carbon position(s) under study ($E_i = p_i$). In case of two-carbon fractions, four possible isotopomers exist: $p^{ij} + p_i^j + p_j^i + p_{ij} = 1$. Similarly to the one-carbon fragments the probability of labeling of two-carbon fragments (p_{ij}) in the metabolic intermediates were calculated based on the scheme of label movement and the flux values obtained from the stoichiometric equation system:

$$p_{ij} = \frac{p_A^{ij} * flux_A + p_B^{ij} * flux_B}{flux_A + flux_B} \quad (16)$$

where p_{ij} - probability of labeling of both carbons i and j , p_A^{ij} and p_B^{ij} - probabilities of labeling of corresponding carbons in precursor molecules A and B, and $flux_A, flux_B$ - corresponding fluxes from the precursor molecules. The probabilities of ^{13}C enrichment in the positions i and j were calculated as follows:

$$p_i = p_{ij} + p_i^j \quad (17)$$

$$p_j = p_{ij} + p_j^i \quad (18)$$

where p_{ij} - probability of ^{13}C labeling in both carbon positions i and j , p_i^j - probability that position i is labeled but j is not labeled, and p_j^i - probability that j is labeled but i is not labeled.

Theoretical conditional enrichments (e.g. the enrichment of carbon i in those molecules where j is also enriched or vice versa) of the two-carbon fragments were calculated as follows:

$$E_i^j = \frac{p_{ij}}{p_{ij} + p_i^j} \quad (19)$$

$$E'_{ij} = \frac{p_{ij}}{p_{ij} + p'_{ij}} \quad (20)$$

In general, the ^{13}C absolute enrichments measured in the labeling experiments are different from the conditional enrichments in the same compound, except for the case when the compound is synthesized in the condensation reaction and different carbon positions under study may originate from the different precursor molecules or different atoms of the same precursor molecule (such as some carbon fragments in isoleucine, leucine, valine, lysine, tyrosine and phenylalanine). In this case:

$$p_{ij} = p_i * p_j \quad (21)$$

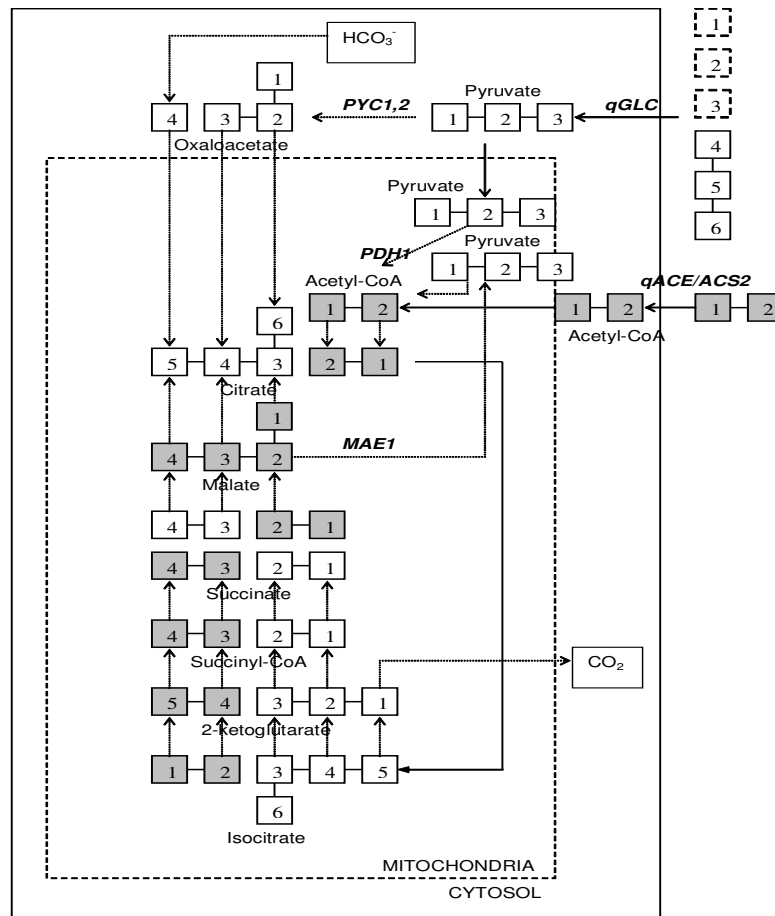


Fig. 14. Incorporation of the label from ^{13}C -[1,2] acetate into the main intermediates of TCA pathway (during the first cycle) in *S. uvarum* grown on the mixed substrates of unlabeled glucose and ^{13}C -[1,2] Na-acetate.

RESULTS AND DISCUSSION

3.1. Metabolic network of *S. uvarum* determined by the ^{13}C labeling and metabolic modeling

The biomass labeling was carried out in D-stat culture with changing culture volume, using two different dilution rates (0.04 h^{-1} and 0.08 h^{-1}) and a substrate containing either ^{13}C -[1,2] Na-acetate and unlabeled glucose, or ^{13}C -[2] Na-acetate and unlabeled glucose. The basic input values for the stoichiometric model (substrate consumption rates and biomass composition) were derived from experimental data (Table 2). Based on the macromolecular composition of biomass determined from the experiments, the concentration of individual monomers and the requirement of NADH and NADPH for their synthesis was calculated based on the literature data (Cortassa et al., 1995), except for those determined experimentally (Appendix II).

Table 2. The basic input values used in the stoichiometric model for the experiments using unlabelled glucose and ^{13}C -[1,2] or ^{13}C -[2] Na-acetate in the dilution media (Paper VI).

	^{13}C -[1,2] Na-acetate	^{13}C -[2] Na-acetate
Absolute and conditional enrichments were calculated from the ^{13}C -NMR spectra of proteogenic amino acids and compared to those calculated from the model (Tables 3 and 4). The label originating from acetate was observed in glutamate, alanine, threonine, aspartate, proline, arginine, lysine, leucine and isoleucine. In the other amino acids the labeling could not be determined due low enrichments (less than 2%), relatively low concentrations, and/or overlapping of the peaks in NMR spectra. In addition, the soluble fraction was extracted from the cells using hot ethanol and analysed for the label incorporation. The ethanol-soluble fraction contained mainly labeled glutamate and trehalose.	0.99	0.99
Dilution rate $[\text{d}^{-1}]$	0.04	0.08
Acetate consumption rate $[\text{Mol} \cdot \text{g}^{-1} \cdot \text{dwt}^{-1}]$	11	7
Glucose consumption rate $[\text{Mol} \cdot \text{g}^{-1} \cdot \text{dwt}^{-1}]$	12	10
Biomass yield $[\text{g} \cdot \text{dwt}^{-1} \cdot \text{g}^{-1} \cdot \text{substrate}^{-1}]$	0.348	0.447
Protein	45	45
Total carbohydrates	30	30
Lipids	1	1
Nucleic acids	5.4	5.4
Ash	8.6	8.6

3.1.1. Biosynthesis of amino acids of glutamate family

Labeling of glutamate in the experiment with ^{13}C -[1,2] acetate is shown in Figure 15. High conditional enrichments calculated from the carbon C_δ and C_γ multiplets (Glu $\text{C}_\gamma^\delta = 92\%$ and Glu $\text{C}_\delta^\gamma = 92\%$) confirm that these fragments were derived almost exclusively from the labeled exogenous acetate. Also other carbons were significantly labeled due to the cycling of α -ketoglutarate (Fig. 14), which is a direct precursor of glutamate. The labeling pattern and ^{13}C enrichments of glutamate as well as other members of the glutamate family (proline and arginine) observed in our labeling experiments (Tables 3 and 4) clearly indicated that the synthesis of α -ketoglutarate was taking place in the mitochondria. If α -ketoglutarate was synthesized outside the mitochondria, enrichments of the glutamate positions C_β , C_γ and C_δ would have been remarkably lower than that observed in our experiments, as the carbons of cytosolic oxaloacetate in applied experimental conditions should be almost exclusively stemmed from unlabeled glucose (Fig. 14). There exists a possibility that α -ketoglutarate can be synthesized through a row of consecutive reactions catalysed by the peroxisomal Cit2p (Lewin et al., 1990), Aco1p (which has been reported of both mitochondrial and cytosolic location), and cytosolic Idp2p or peroxisomal Idp3p (Loftus et al., 1994, Henke et al., 1998). However, the labeling pattern of glutamate cannot directly discriminate between the three possible routes of glutamate synthesis from mitochondrial α -ketoglutarate by 1) mitochondrial

NADH-dependent Glt1p, 2) mitochondrial NADPH-dependent Gdh3p, and 3) cytosolic NADPH-dependent Gdh1p. In case where glutamate synthesis was carried out by cytosolic Gdh1p effective transport of α -ketoglutarate from mitochondria should be involved. Such mitochondrial carrier for α -ketoglutarate is well known (Nałęcz et al. 1986). On the other hand, if glutamate was synthesized using Gdh3p, significant amounts of NADPH should be synthesized in the mitochondria. There are three reactions where NADPH can be derived in mitochondria: 1) reaction catalysed by the mitochondrial NADP-specific isocitrate dehydrogenase (Idp1p), 2) reaction catalysed by the mitochondrial NADP-dependent acetaldehyde dehydrogenases (Ald4p, Ald5p) and 3) reaction catalysed by the mitochondrial malic enzyme (Mae1p). The Ald4p and Ald5p are functional during fermentative metabolism, and because of the high NADPH/NADP ratio compared to the NADH/NAD Idp1p has been reported to be incapable of participating in TCA-based respiration despite its mitochondrial location (Haselbeck and McAlister-Henn, 1991). Thus, their contribution to the mitochondrial NADPH production is negligible and the main NADPH-producing reaction in mitochondria, under specified experimental conditions, was considered to be the oxidative decarboxylation of malate to pyruvate, catalyzed by mitochondrial Mae1p (Boles et al., 1998).

Considering the balance of NADPH in mitochondria, the synthesis of glutamate by mitochondrial NADH-dependent Glt1p would have advantages over NADPH-dependent Gdh3p. In this case the mitochondrial NADPH is only required for the synthesis of the carbon skeleton of valine, leucine, isoleucine and arginine, i.e. the requirement of NADPH for the biosynthesis of other amino acids in mitochondria, where glutamate is also participating, is excluded. When the flux through Mae1p in the model was made or set to be equal to NADPH requirement for the synthesis of valine, leucine, isoleucine and arginine, the ^{13}C enrichments of alanine and valine correlated well with theoretically calculated enrichments of mitochondrial pyruvate, which is the direct precursor of these two amino acids (Tables 3 and 4). On the contrary, when NADPH requirement for the synthesis of glutamate was also included in the model, the calculated theoretical absolute ^{13}C enrichments of mitochondrial pyruvate were 2.5 to 3 times higher than the experimentally determined enrichments of valine and alanine carbons (not illustrated). This suggests that under the given experimental conditions glutamate is either synthesized by mitochondrial Glt1p or cytosolic Gdh1p, and at least part of the pyruvate in the mitochondria should be derived from malate, which is synthesized in the TCA cycle from α -ketoglutarate (Fig. 16).

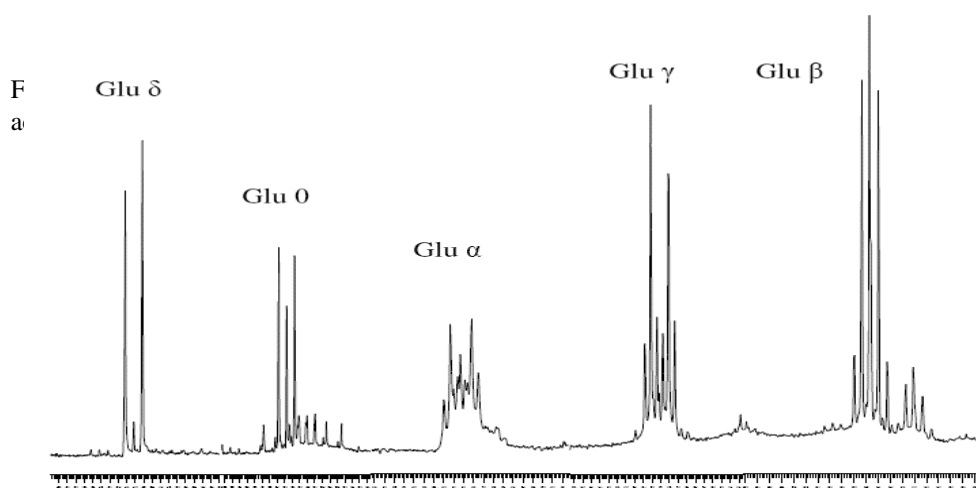


Table 3. Absolute and conditional enrichments of the proteinogenic amino acids determined from the labeling experiment with ^{13}C -[1,2] Na-acetate (99 %) and those calculated from the model (Paper VI).

Precursor carbon	^{13}C enrichments determined from the labeling experiment (%)	^{13}C enrichments calculated from the model (%)
AceCoA _C C ₀	Lys C ₀ =98	99
AceCoA _C C _α	Lys C _α =97	99
AceCoA _m C _α	Leu C _α =42	42
oxa _C C ₀		1.1
oxa _m C ₀	Thr C ₀ =28 Ile C ₀ =30	29
oxa _C C _α		1.1
oxa _m C _α	Thr C _α =31 Ile C _α =33	29
oxa _C C _β		1.1
oxa _m C _β	Thr C _β =32 Ile C _{γ1} =24	29
oxa _C C _γ		23
oxa _m C _γ	Asp C _γ =32 Thr C _γ =35 Ile C _δ =32	33
Pyr _C C _α		1.1
Pyr _m C _α	Ala C _α =5 Leu C _β =5 Val C _α =5 Val C _β =7 Ile C _β =7	5
Pyr _C C _β		1.1
Pyr _m C _β	Ala C _β =7 Leu C _{δ1} =6 Leu C _{δ2} =6 Val C _{γ1} =6 Val C _{γ2} =5 Ile C _{γ2} =4	5
2kg _m C ₀	Glu C ₀ =36	33
2kg _m C _α	Glu C _α =28 Lys C _β =35	29
2kg _m C _β	Arg C _β =33 Lys C _γ =29	29
2kg _m C _γ	Arg C _γ =37 Pro C _γ =35 Lys C _δ =42	42
2kg _m C _δ	Arg C _δ =42 Pro C _δ =37 Lys C _ε =43	42
AceCoA _C C _α ⁰	Lys C _α ⁰ =99	99
AceCoA _C C ₀ ^α	Lys C ₀ ^α =99	99
AceCoA _m C _α ⁰	Leu C _α ⁰ =93	94
oxa _C C _α ⁰		1.1
oxa _m C _α ⁰	Asp C _α ⁰ =68 Thr C _α ⁰ =68 Ile C _α ⁰ =68	69
oxa _C C ₀ ^α		1.1
oxa _m C ₀ ^α	Asp C ₀ ^α =74	69
oxa _C C _β ^γ		1.1
oxa _m C _β ^γ	Thr C _β ^γ =64 Ile C _{γ1} ⁰ =64	61
oxa _C C _γ ^β		23
oxa _m C _γ ^β	Ile C _δ ^{γ1} =62	69
Pyr _m C _α ⁰	Ala C _α ⁰ =54 Val C _α ⁰ =54	58
Pyr _m C _α ^β	Ala C _α ^β =33 Leu C _γ ^{δ1} =34 Val C _β ^{γ1} =33 Ile C _β ^{γ2} =31	29
2kg _m C _α ⁰	Glu C _α ⁰ =58 Pro C _α ⁰ =61 Arg C _α ⁰ =61	61
2kg _m C ₀ ^α	Glu C ₀ ^α =73	69
2kg _m C _β ^γ	Glu C _β ^γ =35 Pro C _β ^γ =26	29
2kg _m C _γ ^δ	Glu C _γ ^δ =92 Pro C _γ ^δ =94 Arg C _γ ^δ =94	94
2kg _m C _δ ^γ	Glu C _δ ^γ =92 Pro C _δ ^γ =87 Arg C _δ ^γ =88	94

Table 4. Absolute and conditional enrichments of the proteinogenic amino acids determined from the labeling experiment with ^{13}C -[2] Na-acetate (90 %) and those calculated from the model (Paper VI).

Precursor carbon	^{13}C enrichments determined from the labeling experiment (%)	^{13}C enrichments calculated from the model (%)
AceCoA _C C ₀	Lys C ₀ =90	90
AceCoA _m C ₀	Leu C ₀ =3	3
AceCoA _m C _α	Leu C _α =28	28
oxa _C C ₀		1.1
oxa _m C ₀	Asp C ₀ =8 Thr C ₀ =6 Ile C ₀ =11	6
oxa _C C _α		1.1
oxa _m C _α	Asp C _α =20 Thr C _α =15 Ile C _α =15	15
oxa _C C _β		1.1
oxa _m C _β	Asp C _β =22 Thr C _β =14 Ile C _β =15	15
oxa _C C _γ		1.1
oxa _m C _γ	Asp C _γ =8 Thr C _γ =7 Ile C _δ =7	8
Pyr _C C ₀		1.1
Pyr _m C ₀	Ala C ₀ =3	2
Pyr _C C _α		1.1
Pyr _m C _α	Ala C _α =3 Leu C _β =2 Val C _α =3 Val C _β =3 Ile C _β =2	4
Pyr _C C _β		1.1
Pyr _m C _β	Ala C _β =3 Leu C _{δ1} =4 Leu C _{δ2} =4 Val C _{γ1} =3 Val C _{γ2} =4 Ile C _{γ2} =4	4
2kg _m C ₀	Glu C ₀ =8 Arg C ₀ =11	8
2kg _m C _α	Glu C _α =16 Arg C _α =11 Lys C _β =18	15
2kg _m C _β	Glu C _β =14 Arg C _β =14 Lys C _γ =14	15
2kg _m C _γ	Glu C _γ =24 Arg C _γ =23 Pro C _γ =25 Lys C _δ =24	28
2kg _m C _δ	Glu C _δ =2 Arg C _δ =4 Pro C _δ =2 Lys C _ε =3	3
oxa _C C _α ⁰		1.1
oxa _m C _α ⁰	Asp C _α ⁰ =16 Thr C _α ⁰ =19	18
oxa _C C ₀ ^α		1.1
oxa _m C ₀ ^α	Asp C ₀ ^α =11 Thr C ₀ ^α =11 Ile C ₀ ^α =11	8
oxa _C C _β ^γ		1.1
oxa _m C _β ^γ	Asp C _β ^γ =15 Thr C _β ^γ =11 Ile C _{γ1} ^δ =13	15
oxa _C C _γ ^β		5
oxa _m C _γ ^β	Ile C _δ ^{γ1} =10	8
Pyr _m C _α ⁰	Ala C _α ⁰ =7	12
Pyr _m C _α ^β	Ala C _α ^β =13 Leu C _γ ^{δ1} =18 Val C _β ^{γ1} =14 Ile C _β ^{γ2} =17	15
2kg _m C _α ⁰	Glu C _α ⁰ =19 Pro C _α ⁰ =20 Arg C _α ⁰ =17	15
2kg _m C ₀ ^α	Glu C ₀ ^α =8	8
2kg _m C _α ^β	Glu C _α ^β =23	19
2kg _m C _β ^α	Glu C _β ^α =16	19
2kg _m C _β ^γ	Glu C _β ^γ =19 Pro C _β ^γ =16 Arg C _β ^γ =16	15
2kg _m C _γ ^β	Glu C _γ ^β =28	28
2kg _m C _γ ^δ	Glu C _γ ^δ =19 Pro C _γ ^δ =19	22
2kg _m C _δ ^γ	Glu C _δ ^γ =5 Pro C _δ ^γ =4 Arg C _δ ^γ =3	3

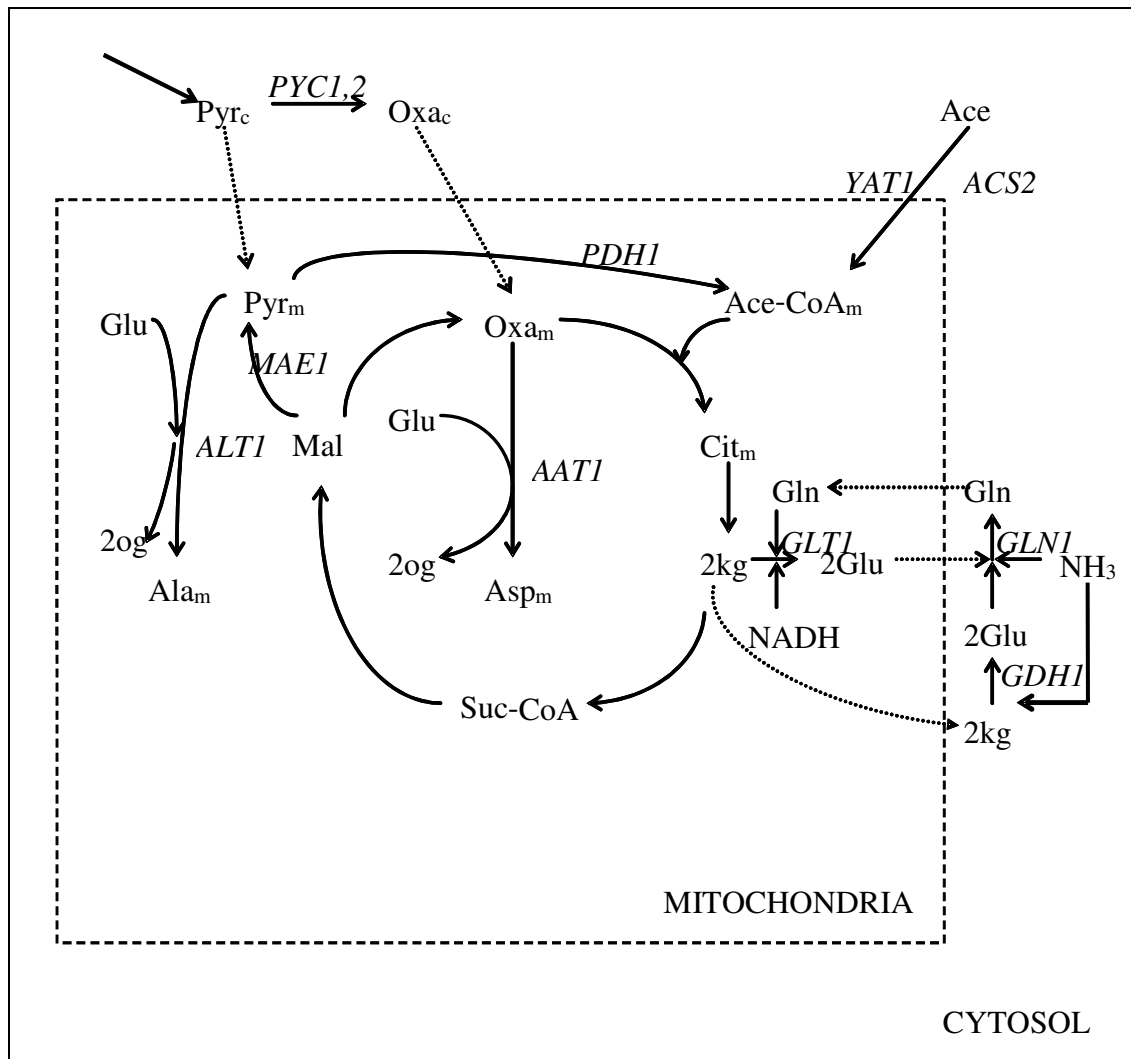


Fig. 16. Metabolic scheme of glutamate, alanine and aspartate biosynthesis in mitochondria. Oxa - oxaloacetate, Cit - citrate, 2kg - α -ketoglutarate, 2og - 2-oxoglutarate, Suc-CoA - succinyl-CoA, Mal - malate, Pyr - pyruvate, Ace - labeled Na-acetate; Glu - glutamate; Gln - glutamine, Ala - alanine, Asp - aspartate. Genes of the enzymes encoding the biosynthetic reactions are given in *italics*, fluxes in and out of the compartments are marked with the dashed arrows.

3.1.2. Biosynthesis of alanine

Alanine is synthesized from pyruvate by the alanine transaminase reaction catalysed in yeast by two enzymes - mitochondrial Alt1p and cytosolic Alt2p (Fig. 6). If alanine was synthesized in the cytosol no labeling could be expected in the given experimental conditions, as cytosolic pyruvate was synthesized mainly from unlabeled glucose (Fig. 14). In addition, the absolute enrichments of alanine C_0 , C_α and C_β from our labeling experiments were very similar to the enrichments of the corresponding carbons of other two amino acids of the pyruvate family - valine and leucine (Fig. 17, Tables 3 and 4), known to be synthesized in mitochondria. Also the same values of conditional enrichments were found for alanine C_α^β , valine $C_\beta^{\gamma 1}$, leucine $C_\gamma^{\delta 1}$ and isoleucine $C_\beta^{\gamma 2}$ representing the same two-carbon fragments of pyruvate. Thus, significantly higher absolute enrichments of alanine (compared to those in glucose and cytosolic pyruvate in the given experimental conditions) can be expected only if mitochondrial pyruvate, labeled with ^{13}C through the Mae1p reaction acts as the alternative precursor for alanine synthesis by mitochondrial Alt1p.

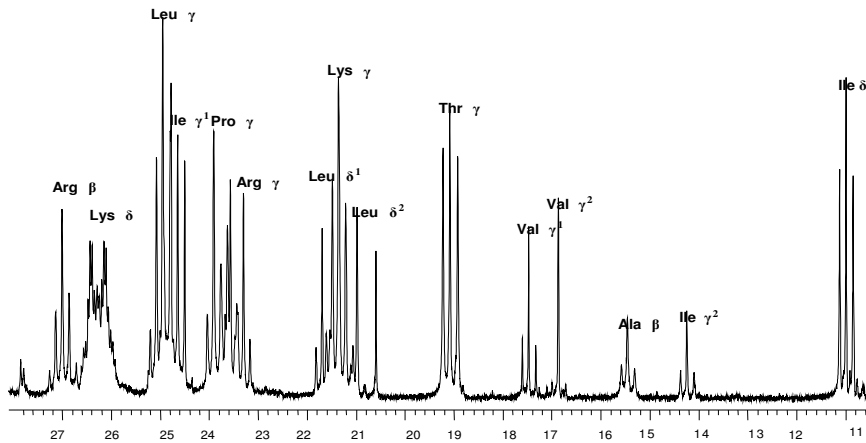


Fig 17. Fraction of the ^{13}C NMR spectra of proteinogenic amino acids from the labeling experiment with ^{13}C -[1,2] Na-acetate.

3.1.3. Biosynthesis of aspartate

The synthesis of aspartate from oxaloacetate may be catalyzed by two aspartate aminotransferases – the mitochondrial Aat1p and cytosolic Aat2p (Fig. 6). The ^{13}C NMR spectra of our labeling experiments indicate that the enrichments of C_0 , C_α and C_β of aspartate and threonine (which is synthesized from aspartate), were remarkably higher than the natural ^{13}C abundance 1.1 % (Tables 3 and 4), which was expected if the cytosolic oxaloacetate derived from unlabeled glycolytic pyruvate was used as the precursor for aspartate synthesis (Fig. 14). As the absolute enrichment of C_γ in aspartate (which derives either from C_γ of malate in mitochondria or CO_2 in cytosol) was also higher than that theoretically calculated for C_γ of cytosolic oxaloacetate, the localization of aspartate synthesis under the given experimental conditions was in mitochondria and the mitochondrial oxaloacetate which was labeled in the TCA cycle over the row of consecutive reactions from acetyl-CoA served as the precursor for aspartate synthesis, catalyzed by the Aatp1 (Fig. 16). This was also confirmed by the higher absolute and conditional enrichments of isoleucine and threonine, the two other amino acids of the aspartate family, where the enrichments of respective carbons showed very good fit with those observed for aspartate (Tables 3 and 4).

3.1.4. Biosynthesis of trehalose

The experiments with ^{13}C labeled Na-acetate and unlabeled glucose at low growth rates resulted in a 4.5 % trehalose concentration in the cells and partial movement of the label into the positions C_γ , C_δ and C_ϵ , while there was no labeling of the positions C_0 , C_α and C_β (Fig. 18). On the contrary to trehalose, no label movement into glycogen was observed.

The incorporation of a label in the presence of glucose can be explained by the oscillations of metabolism due the cell cycle. In the synchronized populations of *S. cerevisiae* the accumulation and mobilization of trehalose has been observed to correlate well with the cell cycle (Küenzi and Fiechter, 1969, Wittmann et al., 2005). As the labeled carbon source in this experiment was ^{13}C -[1,2] Na-acetate, it was supposed that the labeling of trehalose occurs via gluconeogenesis, however in this case equal enrichment of carbons C_0 and C_ϵ , C_α and C_δ , and C_β and C_γ would be expected (Fig. 19A). Upon further analysis, the label movement through the gluconeogenesis pathway reveals that the labeling of carbon positions C_γ , C_δ and C_ϵ in trehalose could be a result of a reaction between seduheptulose-7-P in the PP pathway with glyceraldehyde-3-P derived from labeled mitochondrial oxaloacetate. This results in the labeling of xylulose-5-P and ribose-5-P in the carbon positions of C_β , C_γ and C_δ , which further passed the set of reactions and caused the labeling of trehalose in the given carbon positions (Fig. 19B).

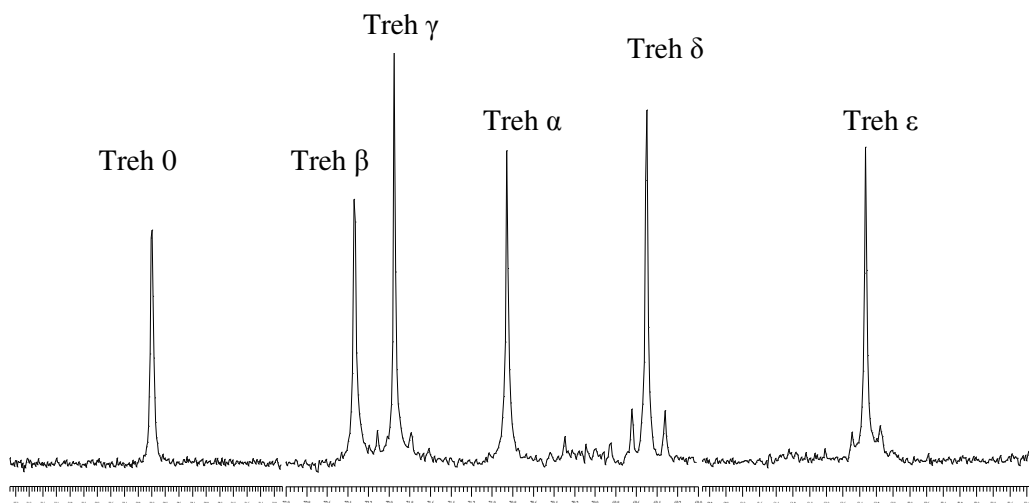


Fig 18. ^{13}C -NMR spectra of trehalose extracted from *S. uvarum* cells grown on glucose and ^{13}C -[1,2] Na-acetate (Paper VI). The low conditional enrichments are observed in trehalose positions C_γ , C_δ and C_ϵ ($\text{C}_\gamma^\epsilon=13\%$ and $\text{C}_\epsilon^\delta=16\%$).

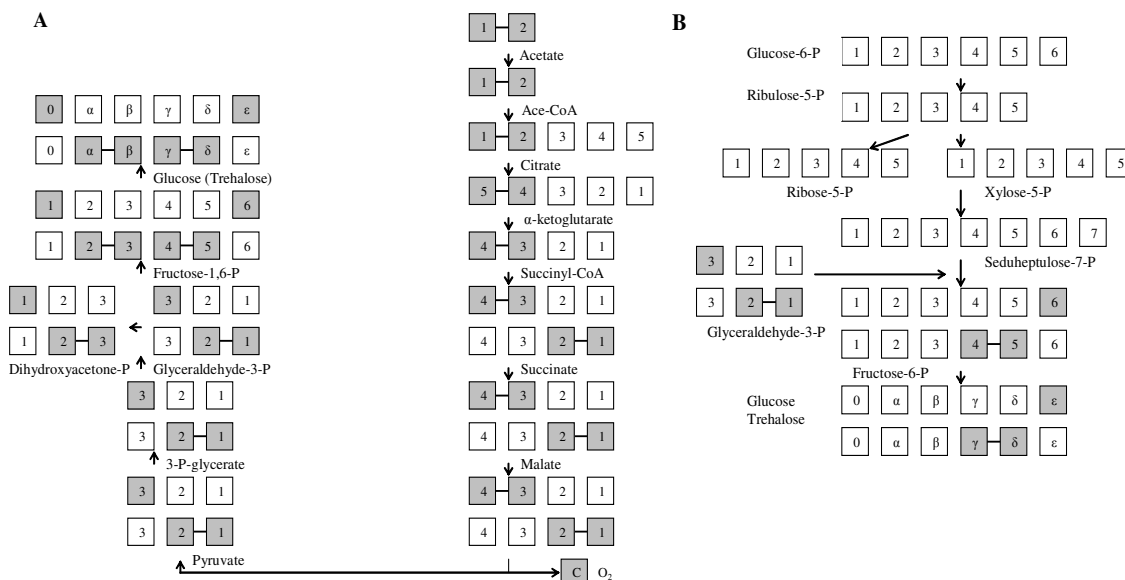


Fig. 19. Predicted label movement from ^{13}C -[1,2] Na-acetate into the carbon positions of trehalose during complete gluconeogenesis (A) and during the proposed shunting through the PP pathway as observed in our labeling experiment (B).

Although the exact reason for such label movement cannot be explained, it was interesting to see that similar shunting of the label through the PP pathway was also proposed by Dickinson et al. (1983) who studied the trehalose synthesis and breakdown in *Pichia pastoris* cells using labeled acetate and glucose. However, despite the clear label movement from acetate into trehalose, as observed in our case, the calculated enrichments do not allow us to claim that acetate was incorporated into trehalose only through the gluconeogenic reactions. According to the scheme of label movement (Fig. 19A,B) the ^{13}C - ^{13}C fragment from acetate can move only into the carbons C_1 and C_2 of 3-phosphoglycerate and thus the coupling lines in C_ϵ of trehalose are not expected (Fig. 18).

3.1.5. Reconstructed metabolic network of *Saccharomyces* spp. for the growth on glucose and acetate

Based on the results of labeling experiments on ^{13}C -[1,2] and ^{13}C -[2] Na-acetate, and unlabeled glucose the modified metabolic network was reconstructed for *Saccharomyces* spp. respiratory growth at low growth rates (Fig. 20). According to the reconstructed metabolic network the metabolite mass balance equation system was composed for the theoretical flux calculations (Appendix I). The calculated flux values were further used to calculate the theoretical absolute and conditional enrichments, which correlate well with the reconstructed metabolic network (Tables 3 and 4). Accordingly, the synthesis of glutamate is catalyzed either by the NADH-dependent glutamate synthase (mitochondrial Glt1p) or glutamate dehydrogenase (cytosolic Gdh1p). Based on the NADPH balance in the mitochondria, as calculated from the model by varying the flux value through the malic enzyme (Mae1p) reaction, the synthesis of glutamate by mitochondrial NADPH-dependent glutamate dehydrogenase (Gdh3p) was excluded. While comparing theoretical calculated enrichments of the carbons of mitochondrial pyruvate with the respective experimental enrichments in valine and alanine, it was found that the major part of NADPH in mitochondria required for synthesis of valine, leucine, isoleucine and arginine was synthesized in the malic enzyme reaction.

There has been some controversy about the exact compartmental location of alanine and aspartate synthesis in *S. cerevisiae*. (Maaheimo et al., 2001; Dos Santos et al., 2003). The labeling pattern from our labeling experiments suggested that alanine and aspartate are both synthesized in the mitochondria by Alt1p and Aat1p respectively. A similar fit for the enrichments of aspartate with the scheme proposed by Maaheimo et al. (2001) where the synthesis of aspartate was in the cytosol, can be obtained only if the mitochondrial barrier for oxaloacetate does not operate or the oxaloacetate flux from mitochondria into cytosol ($\text{OAC1}_{\rightarrow\text{c}}$) is remarkably higher than the resulting flux $\text{OAC1}=\text{OAC1}_{\rightarrow\text{m}}+\text{OAC1}_{\leftarrow\text{m}}$. This is, however, unlikely during fully respiratory growth.

The reversible flux of oxaloacetate between the two compartments cannot, however, be completely excluded as in the given experimental conditions, where Na-acetate was used in addition to glucose the label movement into the trehalose positions C_{γ} , C_{δ} and C_{ϵ} was observed, although to small extent and with an unexpected labeling pattern. According to the pathway analysis, the label could come from mitochondrial oxaloacetate, which was converted into phosphoenolpyruvate in the cytosol by the glyconeogenic enzyme phosphoenolpyruvate (PEP) carboxykinase (Pck1p), followed by conversion into glyceraldehyde-P which was shunted through the PP pathway for unknown reasons. An alternative explanation for the intercompartmental flux of oxaloacetate could be the reversible flux of labeled pyruvate from mitochondria to cytosol, and further conversion to PEP over oxaloacetate. Discrimination between these two possible routes cannot be made based on the labeling pattern and enrichments observed. Despite the probable partial movement of either labeled oxaloacetate or pyruvate from the mitochondria to the cytosol, the labeling pattern and high conditional enrichments of alanine, valine, leucine isoleucine, aspartate and threonine, which correlate well with the metabolic modeling results, support the conclusion that alanine and aspartate synthesis under our experimental conditions was still taking place in the mitochondria.

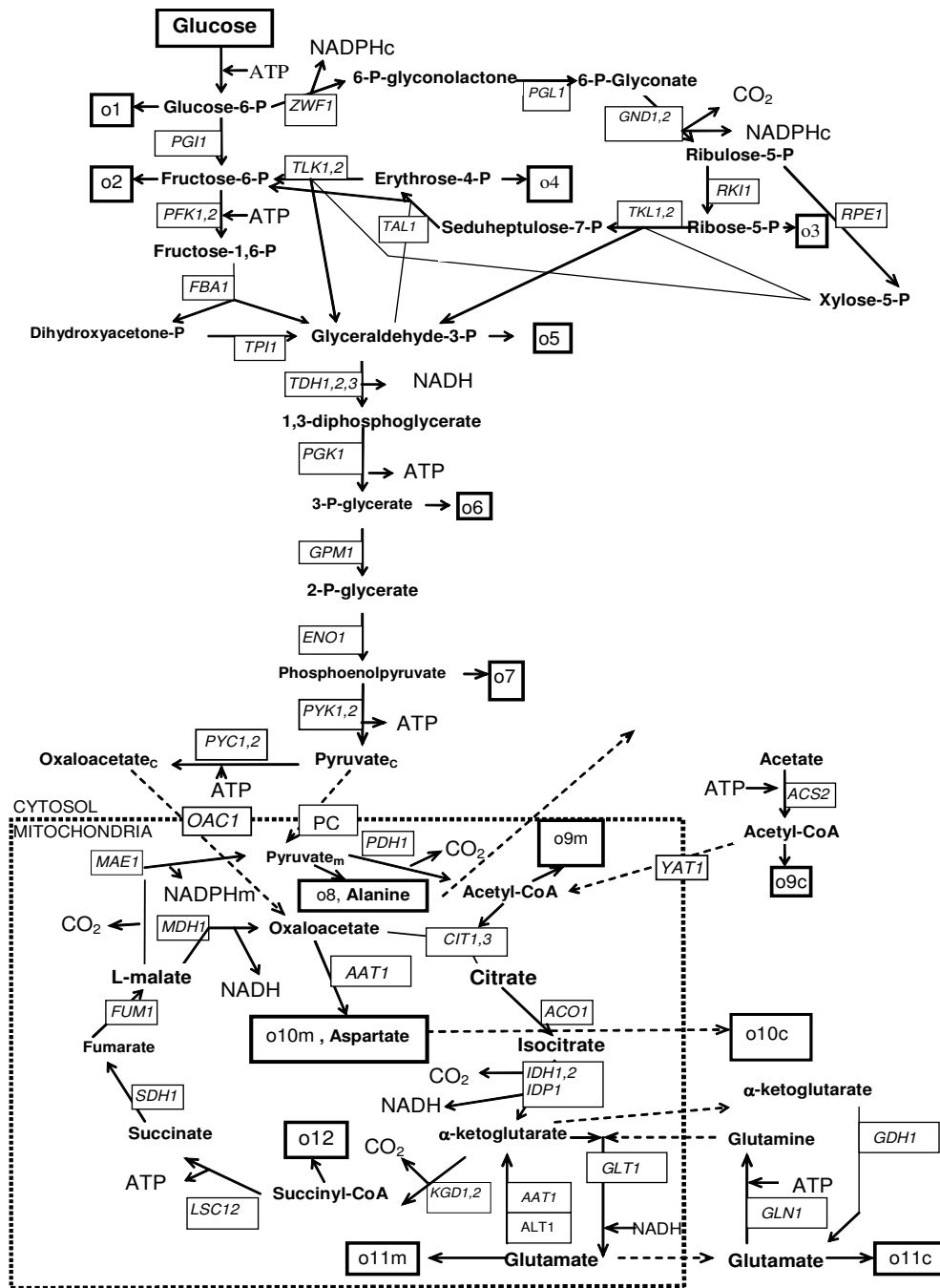


Fig. 20. Metabolic network of active pathways in *S. uvarum* grown on glucose and acetate (Paper VI). Fluxes into the intermediates are given in italics, expressed as the gene abbreviation catalyzing the reaction; fluxes leading to the biomass components (Cortassa, 1995) are expressed as o_i : o_1 , glycogen, glucans, trehalose; o_2 , peptidoglucans, mannans; o_3 , His, dAMP, dGMP, dUMP and dCMP; o_4 , Phe, Trp and Tyr; o_5 , glycerolphosphate; o_6 , Cys, Gly, Ser, dAMP and dGMP; o_7 , Phe, Trp and Tyr; o_8 , Ala, Ile, Leu and Val; o_{9c} , Lys, lauric acid, palmitoleic acid and oleic acid; o_{9m} , Leu; o_{10m} , Asp and Ile; o_{10c} , Met, Thr, Asn, dUMP and dCMP; o_{11m} , Glu and Arg; o_{11c} , Gln, Pro and Lys; o_{12} , heme compounds. Fluxes between the compartments are marked with dashed arrows.

3.2. Expression of the LEA-like protein Hsp12p during the smooth change of stress conditions

Auxo-accelerostat cultivations with either a smooth increase of cultivation temperature or NaCl concentration in the cultivation media were used to study the stress response of yeast *Saccharomyces cerevisiae* by monitoring the expression of the LEA-like protein Hsp12p by measuring fluorescence in a fusion protein construct with *HSP12* as a promoter and *GFP2* as a reporter gene.

The effect of smoothly increasing NaCl concentration on the stress response was compared with the NaCl shift-up experiments carried out in the shake flasks in a culture withdrawn from the fermenter before the onset of the increase of NaCl concentration. The level of expression of the Hsp12p-Gfp2p in the cells (as determined by the fluorescence intensity) in auxo-accelerostat experiments was 50-65 % of that observed in the shift-up experiments with the same concentration of NaCl (Table 5, Fig. 21). The specific rate of Hsp12p-Gfp2p synthesis in auxo-accelerostat increased with increasing NaCl concentration but was more than three fold lower in comparison with the synthesis rate during the first hour of the shift-up experiments. The specific growth rate, as well as specific ethanol production rate decreased with increasing NaCl concentration. The glycerol production rate (not illustrated) and glycerol to ethanol formation ratio (Y_{GE}) started to increase at the NaCl concentrations over 400 mM. The increasing Y_{GE} value correlates well with the increase of the specific Hsp12p-Gfp2p synthesis rate. The observed increase of glycerol and Hsp12p synthesis at higher NaCl concentrations confirms the earlier findings that the expression of the genes of glycerol-3-P dehydrogenase (*GPD1*), glycerol phosphatase (*GPP1*, *GPP2*) and *HSP12* are induced by the high osmolarity glycerol (HOG) pathway (Varela et al., 1995; Akhtar et al., 1997). The results indicate that osmotic stress by NaCl, which caused the decrease in the specific growth rate, is related to an increased synthesis rate of stress-responsive proteins. However, the synthesis of stress-responsive proteins themselves is rather the result than the cause of the observed decrease in growth rate. Most likely, the high NaCl concentrations directly affect the rate of biosynthetic reactions, which through the feedback mechanisms of ATP synthesis, decrease the growth rate as well as the ethanol production rate.

Similarly in the experiment with smoothly increased NaCl concentration, the effect of increasing temperature on the expression of Hsp12p was studied in the auxo-accelerostat cultivation with programmed gradual temperature increase. The shift-up experiments were also performed in parallel in a culture withdrawn from the turbidostat culture before start of the smooth increase of the cultivation temperature. The significant increase in Gfp2p fluorescence in the cells was detected in the shift-up experiments from 30 to 35 and 37°C (Table 5, Fig. 22), which was different from the smooth increase in auxo-accelerostat from 30 to 35 °C (no increase in the fluorescence was observed). With further increase of temperature in auxo-accelerostat over 35 °C significant increase in Hsp12p-Gfp2p synthesis rate occurred, which obtained its maximum at 41 °C. The specific growth rate and ethanol production rate, after obtaining their maximum value at 35°C, remained constant up to 38 °C, after which they started to decrease rapidly (Fig. 22). As temperatures lower than 35°C cause only minor stress to yeast cells, a four fold lower specific synthesis rate of Hsp12p-Gfp2p was observed during the shift-up from 30 to 35°C compared to the shift-up from 30 to 37 °C (Table 5). The glycerol to ethanol formation ratio remained constant up to a cultivation temperature of 39 °C and then started to increase rapidly together with an increase in Hsp12p-Gfp2p synthesis rate at higher cultivation temperatures. The calculated specific Hsp12p-Gfp2p synthesis rate in the shift-up experiment from 30 to 35°C was more than 6 fold higher than that observed in the auxo-accelerostat culture at 35°C. The specific synthesis rate of Hsp12p-Gfp2p calculated for the shift-up experiment from 30 to 37 °C was more than ten fold higher than in the auxo-accelerostat at the same temperature. The results suggest that at temperatures higher than 35 °C damages to the macromolecular biosynthetic apparatus occur, and do not allow the growth rate to follow an Arrhenius plot. These damages may probably induce the synthesis of heat shock proteins through the specific molecular mechanisms acting as the chaperons in the repair of molecular structure of intracellular bioactive compounds and are thus required for maintenance of cell growth.

Table 5. Effect of the NaCl and temperature shift-up on the expression of Hsp12p (as quantitated by the fluorescence intensity) (Paper VII).

	0 min	60 min	Hsp _s	120 min	HSP _s	180 min	Hsp _s
NaCl _{100mM}	137	300	163	308	8	270	-38
NaCl _{400mM}	137	1006	869	851	-155	828	-23
NaCl _{800mM}	137	1136	999	1189	53	1046	-143
T _{35°C}	249	740	491	697	-43	686	-11
T _{37°C}	249	2255	2006	2873	618	3000	127

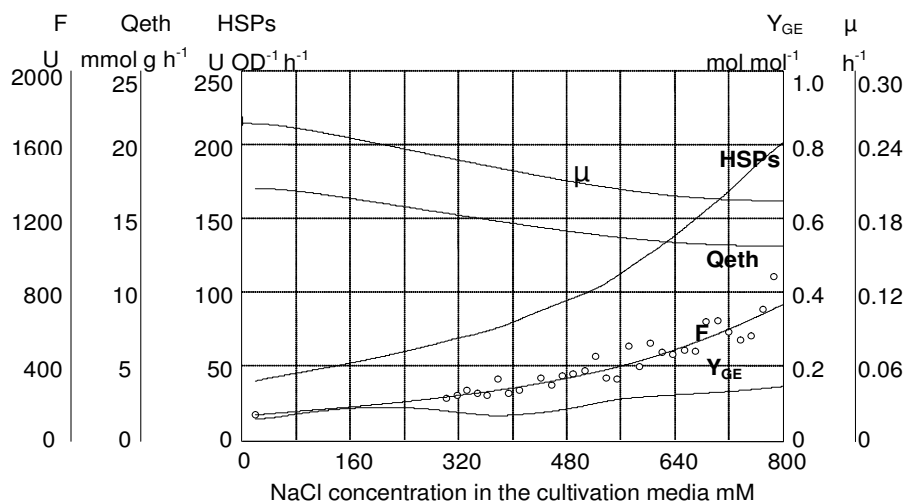


Fig. 21. Auxo-accelerostat cultivation of *S. cerevisiae* Hsp12p-Gfp2p fusion protein construct with a smooth increase of NaCl concentration in the cultivation media (Paper VII). F – specific fluorescence intensity of Gfp2p (in arbitrary units); Qeth – specific ethanol production rate; HSPs – specific Hsp12p-Gfp2p fusion protein synthesis rate in the cells (in arbitrary units per OD unit); Y_{GE} – glycerol to ethanol formation ratio; μ - specific growth rate.

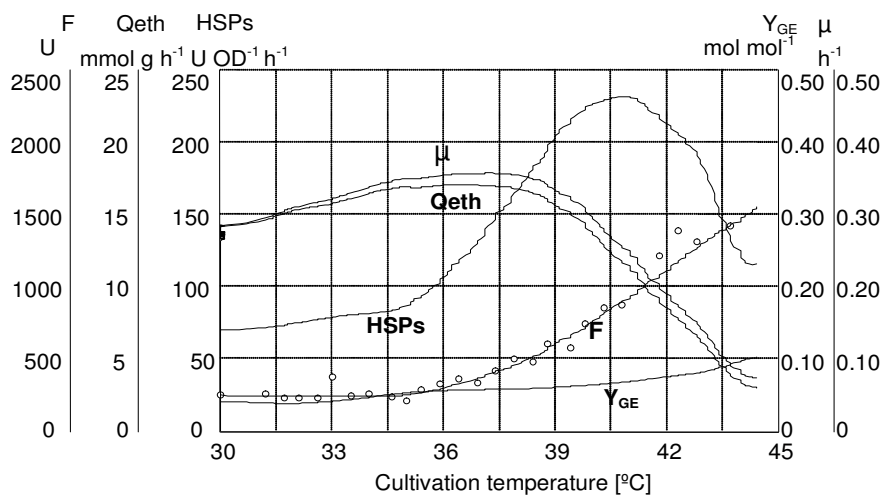


Fig. 22. Auxo-accelerostat cultivation of *S. cerevisiae* Hsp12p-Gfp2p fusion protein construct with a smooth increase of cultivation temperature (Paper VII). F – fluorescence intensity of Gfp2p (in arbitrary units); Qeth – specific ethanol production rate; HSPs – specific synthesis rate of Hsp12p-Gfp2p fusion protein in the cells (in arbitrary units per OD unit); Y_{GE} – glycerol to ethanol formation ratio; μ - specific growth rate.

CONCLUSIONS

1. The absolute and conditional enrichments of cellular metabolites can be well predicted on the basis of metabolic network, biomass composition, specific substrate consumption rates and product formation rates.
2. D-stat culture with mixed substrates (for example unlabeled glucose and ^{13}C -labeled acetate) is an efficient tool for ^{13}C metabolic flux analysis.
3. Our reconstruction of the metabolic network for brewer's yeast *Saccharomyces uvarum* W34 (Fig. 20) based on the contemporary genome databases, information available in the literature and ^{13}C metabolic flux analysis, indicates that under our applied cultivation conditions:
 - a) the synthesis of aspartate is catalyzed by the mitochondrial aspartate aminotransferase (Aat1p);
 - b) the synthesis of alanine is catalyzed by the mitochondrial alanine transaminase (Alt1p);
 - c) the NADPH required for the synthesis of biomass components in mitochondria is derived from the reaction catalyzed by malic enzyme (Mae1p);
 - d) the synthesis of glutamate is catalyzed either by the mitochondrial NADH-dependent glutamate synthase (Glt1p) or cytosolic NADH-dependent glutamate dehydrogenase (Gdh1p) but not by the mitochondrial NADPH-dependent glutamate dehydrogenase (Gdh3p).
4. The expression rate of Hsp12p as a response to environmental stress conditions, such as higher temperature and osmotic pressure, depends more significantly on the rate of change of the stress condition than on the stress condition itself.
5. The continuous cultivation methods with controlled change rate of an environmental parameter (D-stat and auxo-accelerostat) using Gfp2p fusion protein constructs for fluorescence labeling are efficient and effective tools for the study of the response of yeast metabolism to progressing stress conditions common to many industrially applied conditions.

REFERENCES

- Abadijeva, A., Pauwels, K., Hilven, P. and Crabeel, M. (2001) The N-acetylglutamate synthase/N-acetylglutamate kinase metabolon of *Saccharomyces cerevisiae* allows coordinated feedback regulation of the first two steps in arginine biosynthesis. *Eur. J. Biochem.* 270, 1014-1024.
- Adamberg, K., Kask, S., Laht, T. M. and Paalme, T. (2003) The effect of temperature and pH on the growth of lactic acid bacteria: a pH-auxostat study. *Int. J. Food Microbiol.* 85, 171-183.
- Akhtar, N., Blomberg, A. and Adler, L. (1997) Osmoregulation and protein expression in a *pbs2Δ* mutant of *Saccharomyces cerevisiae* during adaptation to hypersaline stress. *FEBS Letters.* 403, 173-180.
- Albers, E., Laizé, V., Blomberg, A., Hohmann, S. and Gustafsson, L. (2003) Ser3p (Yer081wp) and Ser33p (Yil074cp) Are Phosphoglycerate Dehydrogenases in *Saccharomyces cerevisiae*. *J. Biol. Chem.* 278, 10264-10272.
- Bailey, J. E. (1998) Mathematical Modeling and Analysis in Biochemical Engineering: Past Accomplishments and Future Opportunities. *Biotechnol. Prog.* 14, 8-20.
- Bell, W., Sun, W., Hohmann, S., Wera, S., Reinders, A., De Virgilio, C., Wiemken, A. and Thevelein, J.M. (1998) Composition and functional analysis of the *Saccharomyces cerevisiae* trehalose synthase complex. *J. Biol. Chem.* 273, 33311-33319.
- Benachenhou-Lahfta, N., Forterre, P. and Labendan, B. (1993) Evolution of glutamate dehydrogenase genes: evidence for two paralogous protein families and unusual branching patterns of the archaeobacteria in the universal tree of life. *J. Mol. Evol.* 36, 335-346
- Betterton, H., Fjellstedt, T., Matsuda, M., Ogur, M. and Date, R. (1968) Localization of the homocitrate pathway. *Biochim. Biophys. Acta.* 170, 459-461
- Blum, J. and Stein, R. (1982) On the analysis of metabolic networks. In R. F. Goldberger (Ed.), *Biological Regulation and Development*. Plenum Press, New York, 99-124.
- Boles, E., Jong-Gubbels, P. and Pronk, J. T. (1998) Identification and Characterization of *MAE1*, the *Saccharomyces cerevisiae* Structural Gene Encoding Mitochondrial Malic Enzyme. *J. Bacteriol.* 180, 2875-2882.
- Bon, E., Neuveglise, C., Casaregola, S., Artiguenave, F., Wincker, P., Aigle, M. and Durrens, P. (2000) Genomic exploration of the hemiascomycetous yeast: 5. *Saccharomyces bayanus* var. *uvarum*. *FEBS Lett.* 487, 37-41.
- Braus, G. H. (1991) Aromatic Amino Acid Biosynthesis in the Yeast *Saccharomyces cerevisiae*: A Model System for the Regulation of a Eucaryotic Biosynthetic Pathway. *Microbiological Reviews.* 55, 349-370.
- Cannizarro, C., Christensen, B., Nielsen, J. and Stockar, U. (2004) Metabolic network analysis on *Phaffia rhodozyma* yeast using ¹³C-labeled glucose and gas chromatography-mass spectrometry. *Metabolic Engineering.* 6, 340-351.
- Chalfie, M., Tu, Y., Euskirchen, G., Ward, W. W. and Parcher, D. C. (1994) Green fluorescence protein as a marker for gene expression. *Science.* 263, 802-805.
- Chen, S., Brockenbrough, J. S., Dove, J. E. and Aris, J. P. (1997) Homocitrate synthase is located in the nucleus in the yeast *Saccharomyces cerevisiae*. *J. Biol. Chem.* 272, 10839-10846.

- Cherry, J. M., Adler, C., Ball, C., Chervitz, S. A., Dwight, S. S., Hester, E. T., Jia, Y., Juvik, G., Roe, T., Schroeder, M., Weng, S. and Botstein D. (1998) SGD: Saccharomyces Genome Database. *Nucleic Acids Res.* 26, 73-79.
- Christensen, B. and Nielsen, J. (2000¹) Metabolic network analysis. A powerful tool in metabolic engineering. *Adv. Biochem. Eng. Biotechnol.* 66, 209-231.
- Christensen, B. and Nielsen, J. (2000²) Metabolic Network Analysis of *Penicillium chrysogenum* Using ¹³C-Labeled Glucose. *Biotechnol. Bioeng.* 68, 652-659.
- Christensen, B., Gombert, A. K. and Nielsen, J. (2002) Analysis of flux estimates based on ¹³C-labelling experiments. *Eur. J. Biochem.* 269, 2795-2800.
- Clancy, M.J., Smith, L. M. and Magee, P. T. (1982) Developmental regulation of a sporulation-specific enzyme activity in *Saccharomyces cerevisiae*. *Mol. Cell. Biol.* 2, 171-178.
- Cortassa, S., Aon, J. C. and Aon, M. A. (1995) Fluxes of carbon, phosphorylation, and redox intermediates during growth of *Saccharomyces cerevisiae* on different carbon sources. *Biotechnol. Bioeng.* 47, 193-208.
- Covert, M. W., Schilling, C. H., and Palsson, B. O. (2001) Regulation of gene expression in flux balance models of metabolism. *J. Theoret. Biol.* 213, 73-88.
- Crabeel, M., Soetens, O., De Rijcke, M., Pratiwi, R. and Pankiewicz, R. (1996) The ARG11 gene of *Saccharomyces cerevisiae* encodes a mitochondrial integral membrane protein required for arginine biosynthesis. *J. Biol. Chem.* 271, 25011-25018.
- Craig, E. A., Weissman, J. S. and Horwich, A. L. (1994) Heat shock proteins and molecular chaperones: mediators of protein conformation and turnover in the cell. *Cell.* 78, 365-372.
- De Deken, R. H. (1966) The Crabtree effect: a regulatory system in yeast. *J. Gen. Microbiol.* 44, 149-156.
- DeJuan, C. and Lagunas, R. (1986) Inactivation of the galactose transport system in *Saccharomyces cerevisiae*. *FEBS Lett.* 207, 258-261.
- DeLuna, A., Avendaño, A., Riego, L., and González, A. (2001) NADP-Glutamate Dehydrogenase Isoenzymes of *Saccharomyces cerevisiae*. *J. Biol. Chem.* 276, 43775-43783.
- DeVit, M. and Johnston, M. (1996) Analysis of the regulation of the Mig1 glucose repressor. *In: Yeast Genetics and Molecular Biology.* Madison, WI, USA. 282-283.
- Dickinson J. R., Dawes I. W., Boyd A. S. and Baxter R. L. (1983). ¹³C NMR studies of acetate metabolism during sporulation of *Saccharomyces cerevisiae*. *Proc. Natl. Acad. Sci. USA.* 80, 5847-5851.
- Domach, M. M. and Shuler, M. L. (1984) A finite representation model for an asynchronous culture of *E. coli*. *Biotechnol. Bioeng.* 26, 877-884.
- Domach, M. M., Leung, S. K., Cahn, R. E., Cocks, G. G. and Shuler, M. L. (1984) Computer model for glucose-limited growth of a single copy of *Escherichia coli* B/r-A. *Biotechnol. Bioeng.* 26, 203-216.
- Dos Santos, M., Gombert, A., Christensen, B., Olsson, L. and Nielsen, J. (2003) Identification of In vivo enzyme Activities in the Cometabolism of Glucose and Acetate by *Saccharomyces cerevisiae* by Using ¹³C-Labeled Substrates. *Eucaryotic Cell.* 2, 599-608.

- Duggleby, R. G. and Pang, S. S. (2000) Acetohydroxyacid synthase. *J. Biochem. Mol. Biol.* 33, 1-36.
- Dunn, I. J. and Mor, J. R. (1975). Variable-volume continuous cultivation. *Biotechnol. Bioeng.* 17, 1805-1822.
- Edwards, J. S., Covert, M. and Palsson, B. (2002) Metabolic modeling of microbes: the flux-balance approach. *Environ. Microbiol.* 4, 133-140.
- Elbein, A. D., Pan, Y. T., Pastuzak, I. and Carroll, D. (2003) New insights on trehalose: a multifunctional molecule. *Glycobiology.* 13, 17R-27R.
- Entian, K. D. and Barnett, J. A. (1992) Regulation of sugar utilization by *Saccharomyces cerevisiae*. *Trends Biochem. Sci.* 17, 506-510.
- Fiechter, A., Fuhrmann, G. F. and Käppeli, O. (1981) Regulation of glucose metabolism in growing yeast cells. *Adv. Microb. Physiol.* 22, 123-183.
- Fiechter, A. and Seghezzi, W. (1992) Regulation of glucose metabolism in growing yeast cells. *J. Biotechnol.* 27, 27-45.
- François, J., Neves, M. J. and Hers, H. G. (1991) The control of trehalose biosynthesis in *Saccharomyces cerevisiae*: evidence for a catabolite inactivation and repression of trehalose-6-phosphate synthase and trehalos-6-phosphate phosphatase. *Yeast.* 7, 575-587.
- François, J. and Parrou, L. (2001) Reserve carbohydrates metabolism in the yeast *Saccharomyces cerevisiae*. *FEMS Microbiol. Rev.* 25, 125-145.
- Frick, O. and Wittmann, C. (2005) Characterization of the metabolic shift between oxidative and fermentative growth in *Saccharomyces cerevisiae* by comparative ¹³C flux analysis. *Microb. Cell Fact.* 4, 30.
- Gancedo, C. (1992) Molecular cloning of *CIF1*, a yeast gene necessary for growth on glucose. *Yeast.* 8, 183-192.
- Förster, J., Famili, I., Fu, P., Palsson, B. O. And Nielsen, J. (2003) Genome-scale reconstruction of the *Saccharomyces cerevisiae* metabolic network. *Genome Res.* 13, 244-253.
- Goffeau, A. (1997) The yeast genome directory. *Nature.* 387, 5-6.
- Guldener, U., Munsterkötter, M., Kastenmüller, G., Strack, N., van Helden, J., Lemer, C., Richelles, J., Wodak, S.J., Garcia-Martinez, J., Perez-Ortin, J. E., Michael, H., Kaps, A., Talla, E., Dujon, B., Andre, B., Souciet, J.L., De Montigny, J., Bon, E., Gaillardin, C. and Mewes, H.W. (2005) CYGD: the Comprehensive Yeast Genome Database. *Nucleic Acids Res.* 33, 364-368.
- Hartman, S. C. and Buchanan, J. M. (1959) Nucleic acids, purines, pyrimidines (nucleotide synthesis). *Annu. Rev. Biochem.* 28, 365-410.
- Haselbeck, R. J. and McAlister-Henn, L. (1991) Isolation, nucleotide sequence, and disruption of the *Saccharomyces cerevisiae* gene encoding mitochondrial NADP(H)-specific isocitrate dehydrogenase. *J. Biol. Chem.* 266, 2339-2345.
- Hasslacher, M., Ivessa, A.S., Paltauf, F. and Kohlwein, S.D. (1996) Acetyl-CoA carboxylase from yeast is an essential enzyme and is regulated by factors that control phospholipid metabolism. *J. Biol. Chem.* 268, 10946-10952.

- Henke, B., Girzalsky, W., Berteaux-Lecellier, V. And Erdmann, R. (1998) IDP3 Encodes a Peroxisomal NADP-dependent Isocitrate Dehydrogenase Required for the β -Oxidation of Unsaturated Fatty Acids. *J. Biol. Chem.* 6, 3702-3711.
- Hinnebusch, A. (1992) General and pathway-specific regulatory mechanisms controlling the synthesis of amino acid biosynthetic enzymes in *Saccharomyces cerevisiae*. In: *The Molecular and Cellular Biology of the yeast Saccharomyces: Gene Expression*. 2, 319-414.
- Hodges, P. E., McKee, A. H., Davis, B. P., Payne, W. E. and Garrels, J. I. (1998) The Yeast Proteome Database: a model for the organization and presentation of genome-wide functional data. *Nucleic Acids Res.* 27, 69-73.
- Holzer, H. and Schneider, S. (1957) Enrichment and separation of a diphosphopyridine nucleotide specific and triphosphopyridine nucleotide specific glutamine acid dehydrogenase from yeast. *Biochem. Z.* 329, 361-369.
- Holzer, H. (1976) Catabolite inactivation in yeast. *Trends Biochem. Sci.* 1, 178-181.
- Hottiger, T., Schmutz, P and Wiemken, A. (1987) Heat-Induced Accumulation and Futile Cycling of Trehalose in *Saccharomyces cerevisiae*. *J. Bacteriol.* Dec, 5518-5522.
- Huh, W. K., Falvo, J. V., Gerke, L. C., Carroll, A. S., Howson, R. W., Weissman, J. S. and O'Shea, E. K. (2003) Global analysis of protein localization in budding yeast. *Nature*. 16, 686-691.
- Jeong, H., Tombor, B., Albert, R., Oltvai, Z. N., Barabasi, A.L. (2000) The large-scale organization of metabolic networks. *Nature*. 407, 651-654.
- Kanehisa M, Goto S, Kawashima S, Okuno Y, Hattori M. (2004) The KEGG resource for deciphering the genome. *Nucleic Acids Res.* 32, 277-280.
- Karreman, R. and Lindsey, G. (2005) A rapid method to determine the stress status of *Saccharomyces cerevisiae* by monitoring the expression of a Hsp12:green fluorescent protein (GFP) construct under the control of the Hsp12 promoter. *J. Biomol. Screen.* 10, 253-259.
- Kellis, M., Patterson, N., Endrizzi, M., Birren, B. and Lander, E.S. (2003) Sequencing and comparison of yeast species to identify genes and regulatory elements. *Nature*. 423, 241-254.
- Klein, C. J., Olsson, L. and Nielsen, J. (1998) Glucose control in *Saccharomyces cerevisiae*: the role of *MIG1* in metabolic functions. *Microbiology*. 144, 13-24.
- Kohlwein, S. D., Daum, G., Schneiter, R. And Paltauf, F. (1996) Phospholipids: synthesis, sorting, subcellular traffic- the yeast approach. *Trends Cell. Biol.* 6, 260-266.
- Kohlwein, S.D. (2000) The beauty of the yeast. Live cell microscopy at the limits of optical resolution. *Microsc. Res. Technol.* 51, 511-529.
- Kumar, A., Agarwal, S., Heyman, J. A., Matson, S., Heidtman, M., Piccirillo, S., Umansky, L., Drawid, A., Jansen, R., Liu, Y., Cheung, K. H., Miller, P., Gerstein, M., Roeder, G. S. and Snyder, M. (2002) Subcellular localization of the yeast proteome. *Genes Dev.* 16, 707-719.
- Kurtzmann, C. and Fell, J. (1997) In: *The Yeasts*, 4th Ed. Elsevier Science.
- Käppeli O. (1986) Regulation of carbon metabolism in *Saccharomyces cerevisiae* and related yeast. *Adv. Microb. Physiol.* 28, 181-209.
- Küenzi, M. and Fiechter, A. (1969) Changes in carbohydrate composition and trehalase activity during the budding cycle of *Saccharomyces cerevisiae*. *Arch. Mikrobiol.* 64, 396-407.

- Küenzi, M. and Fiechter, A. (1972) Regulation of carbohydrate composition of *S. cerevisiae* under growth limitation. *Arch. Mikrobiol.* 84, 254-265.
- Lafaye, A., Labarre, J., Tabet, J. C., Ezan, E. and Junot, C. (2005) Liquid chromatography-mass spectrometry and ¹⁵N metabolic labeling for quantitative metabolic profiling. *Anal Chem.* 77, 2023-2033.
- Lewin, A. S., Hines, V. and Small, G. M. (1990) Citrate Synthase Encoded by the *CIT2* Gene of *Saccharomyces cerevisiae* Is Peroxisomal. *Mol. Cell. Biol.* 10, 1399-1405.
- Li, W. and Brandriss, M. C. (1992) Proline biosynthesis in *Saccharomyces cerevisiae*: molecular analysis of the *PRO1* gene, which encodes gamma-glutamyl kinase. *J. Bacteriol.* 174, 4148-4156.
- Loftus, T. M., Hall, L. V., Anderson, S. L. and McAlister-Henn, L. (1994) Isolation, characterization, and disruption of the yeast gene encoding cytosolic NADP-specific isocitrate dehydrogenase. *Biochemistry.* 16, 9661-9667.
- Maaheimo, H., Fiaux, J., Çakar, Z. P., Bailey, J., Sauer, U. and Szyperski, T. (2001) Central carbon metabolism of *Saccharomyces cerevisiae* explored by biosynthetic fractional ¹³C labeling of common amino acids. *Eur. J. Biochem.* 268, 2464-2479.
- Magasanik, B. (2003) Ammonia Assimilation by *Saccharomyces cerevisiae*. *Eukaryotic cell.* Oct., 827-829.
- Mager, W. H. and Ferreira, P. M. (1993) Stress response of yeast. *Biochem. J.* 290, 1-13.
- Mager, W. H. and De Kruijff, A. J. (1995) Stress-Induced Transcriptional Activation. *Microbiol. Rev.* Sept., 506-531.
- Malloy, C., Sherry, A. and Jeffrey, F. (1988) Evaluation of carbon flux and substrate selection through alternate pathways involving the citric acid cycle of the heart by ¹³C NMR spectroscopy. *J. Biol. Chem.* 263, 6964-6971.
- Masselot, M. and De Robichon-Szulmajster, H. (1975) Methionine biosynthesis in *Saccharomyces cerevisiae*. I. Genetical analysis of auxotrophic mutants. *Mol. Gen. Genet.* 139, 121-132.
- Mateus, C. and Avery, S. V. (2000) Destabilized green fluorescent protein for monitoring dynamic changes in yeast gene expression with flow cytometry. *Yeast.* 16, 1313-1323.
- Matsuyama, A., Arai, R., Yashiroda, Y., Shirai, A., Kamata, A., Sekido, S., Kobayashi, Y., Hashimoto, A., Hamomato, M., Hiraoka, Y., Horinouchi, S. and Yoshida, M. (2006) ORFeome cloning and global analysis of protein localization in the fission yeast *Schizosaccharomyces pombe*. *Nature Biotechnol.* 24, 841-847.
- Melcher, K. and Entian, K. D. (1992) Genetic analysis of serine biosynthesis and glucose repression in yeast. *Curr. Genet.* 21, 295-300.
- Michal, G. (1998) *In: Biochemical Pathways: an Atlas of Biochemistry and Molecular Biology.* Wiley, New York.
- Morin, P., Subramanian, G. and Gilmore, T. (1992) *AAT1*, a gene encoding a mitochondrial aspartate aminotransferase in *Saccharomyces cerevisiae*. *Biochim. Biophys. Acta.* 1171, 211-214.

- Motshwene, P., Karreman, R., Kgari, G., Brandt, W. And Lindsey, G. (2004) LEA (late embryonic abundant)-like protein Hsp12 (heat-shock protein 12) is present in the cell wall and enhances the barotolerance of the yeast *Saccharomyces cerevisiae*. *Biochem. J.* 377, 769-774.
- Nałęcz, J. M., Nałęcz, K. A., Broger, C., Bolli, R., Wojtczak, L. and Azzi, A. (1986) Extraction, partial purification and functional reconstitution of two mitochondrial carriers transporting keto-acids: 2-oxoglutarate and pyruvate. *FEBS Lett.* 196, 331-336.
- Nguyen, H-V. and Gaillardin, C. (2005) Evolutionary relationships between the former species *Saccharomyces uvarum* and the hybrids *Saccharomyces bayanus* and *Saccharomyces pastorianus*; reinstatement of *Saccharomyces uvarum* (Beijerinck) as a distinct species. *FEMS Yeast Res.* 5, 471-483.
- Nwaka, S., Mechler, B., Destruelle, M. and Holzer, H. (1995) Phenotypic features of trehalase mutants in *Saccharomyces cerevisiae*. *FEBS Lett.* 360, 286-290.
- Ono, B., Shirahige, Y., Nanjoh, A., Andou, N., Ohue, H. and Ishino-Arao, Y. (1988) Cysteine biosynthesis in *Saccharomyces cerevisiae*: mutation that confers cystathionine beta-synthase deficiency. *J. Bacteriol.* 170, 5883-5889.
- Paalme, T., Olivson, A. and Vilu, R. (1982¹) ¹³C-NMR study of the glucose synthesis pathways in the bacterium *Chlorobium thiosulfatophilum*. *Biochim. Biophys. Acta.* 720, 303-310.
- Paalme, T., Olivson, A. and Vilu, R. (1982²) ¹³C-NMR study of CO₂-fixation during the heterotrophic growth in *Chlorobium thiosulfatophilum*. 1982. *Biochim. Biophys. Acta.* 782, 311-319.
- Paalme, T., Tiisma, K., Kahru, A., Vanatalu, K. And Vilu, R. (1990) Glucose-limited Fed-Batch Cultivation of *Escherichia coli* with Computer-Controlled Fixed Growth Rate. *Biotechnol. Bioeng.* 35, 312-319.
- Paalme T., Elken R., Vilu R. and Korhola M. (1997) Growth efficiency of *Saccharomyces cerevisiae* on glucose/ethanol media with a smooth change in dilution rate (A-stat). *Enzyme Microb. Technol.* 20, 174–181.
- Parsell, D. A., Kowal, A. S., Singer, M. A. and Lindquist, S. (1994) Protein disaggregation mediated by heat shock protein Hsp104. *Nature.* 372, 475-478.
- Piper, P. W., Talreja, K., Panaretou, B., Moradas Ferreira, P., Byrne, K., Preakelt, U. M., Meacock, P., Récnacq, M. and Boucherie, H. (1994) Induction of major heat shock proteins of *Saccharomyces cerevisiae*, including plasma membrane Hsp30, by ethanol levels above a critical treshold. *Microbiology.* 140, 3031-3038.
- Pitkänen, J. P. (2005) Impact of Xylose and Mannose on Central Metabolism of Yeast. *In: Doctoral Theses of Helsinki University of Technology, Espoo, Finland.*
- Prasher, D. C., Eckenrode, V. K., Ward, W. W., Prendgast, F. G. and Gormier, M. J. (1992) Primary structure of the *Aequorea victoria* green-fluorescent protein. *Gene.* 111: 229-233.
- Rep, M., Albertyn, J., Thevelein, J. M., Prior, B. A. and Hohmann, S. (1999) Different signaling pathways contribute to the control of *GPD1* gene expression by osmotic stress in *Saccharomyces cerevisiae*. *Microbiology.* 145, 715-727.
- Rizzuto, R., Brini, R., Pizzo, P., Murgia, M. and Pozzan, T. (1995) Chimeric green fluorescent protein as a tool for visualizing subcellular organelles in living cells. *Current Biology.* 5, 635-642.

- Roon, R.J., Even, H.L., and Larimore, F. (1974) Glutamate synthase: properties of the reduced nicotinamide adenine dinucleotide-dependent enzyme from *Saccharomyces cerevisiae*. *J. Bacteriol.* 118, 89-95.
- Ross-Macdonald, P., Sheehan, A., Roeder, G. S. and Snyder, M. (1997) A multipurpose transposon system for analyzing protein production, localization, and function in *Saccharomyces cerevisiae*. *Proc. Natl Acad. Sci. USA.* 94, 190–195.
- Ryan, E.D., Tracy, J.W. and Kohlhaw, G.B. (1973) Subcellular localization of the leucine biosynthetic enzymes in yeast. *J. Bacteriol.* 116, 222-225.
- Ryan, E. D. and Kohlhaw, G. B. (1974) Subcellular localization of the isoleucine-valine biosynthetic enzymes in yeast. *J. Bacteriol.* 120, 631-637.
- Sales, K., Brandt, W. F., Rumbak, E. and Lindsey, G. G. (2000) The LEA-like protein Hsp12 in *Saccharomyces cerevisiae* has a plasma membrane location and protects membranes against desiccation and ethanol-induced stress. *Biochim. Biophys. Acta.* 1463, 267-278.
- Sanchez, Y. and Lindquist, S.L. (1990) HSP104 required for induced thermotolerance. *Science.* 248, 1112-1115.
- Schilling, C. H and Palsson, B. O. (2000) Assessment of the metabolic capabilities of *Haemophilus influenzae* Rd through a genome-scale pathway analysis. *J. Theor. Biol.* 203, 249-283.
- Schlosser, T., Gatens, C., Weber, U. and Stahmann, K. P. (2004) Alanine:glyoxylate aminotransferase of *Saccharomyces cerevisiae*-encoding gene *AGX1* and metabolic significance. *Yeast* 21, 63-73.
- Schüller, H-J. (2003) Transcriptional control of nonfermentative metabolism in yeast. *Current Genetics.* 43, 139-160.
- Sickmann, A., Reinders, J., Wagner, Y., Joppich, C., Zahedi, R., Meyer, H. E., Schonfisch, B., Perschil, I., Chacinska, A., Guiard, B., Rehling, P., Pfanner, N. and Meisinger, C. (2003) The proteome of *Saccharomyces cerevisiae* mitochondria. *Proc. Natl. Acad. Sci. USA.* 100, 13207-13212.
- Siderius, M., Rots, E. and Mager, W. H. (1997) High-osmolarity signaling in *Saccharomyces cerevisiae* is modulated in a carbon-source-dependent fashion. *Microbiology.* 143, 3241-3250.
- Sinclair, D. A. and Dawes, I. E. (1995) Genetics of the Synthesis of Serine from Glycine and the Utilization of Glycine as Sole Nitrogen Source by *Saccharomyces cerevisiae*. *Genetics.* 140, 1213-1222.
- Siro, M. R. and Lövgren, T. (1978) On the properties of α -glucosidase and the binding of glucose to the enzyme. *Org. Chem. Biochem.* 32, 447-451.
- Straight, A. F., Belmont, A. S., Robinett, C. C. and Murray, A. W. (1996) GFP tagging of budding yeast chromosomes reveals that protein-protein interactions can mediate sister chromatid cohesion. *Curr. Biol.* 6, 1599-1608.
- Sunnarborg, S. W., Miller, S. P., Unnikrishnan, I. and LaPorte, D. C. (2001) Expression of the yeast glycogen phosphorylase gene is regulated by stress-response elements and by the HOG MAP kinase pathway. *Yeast.* 18, 1505-1514.
- Szyperski, T., Bailey, J. and Wütrich, K. (1996) Detecting and dissecting metabolic fluxes using biosynthetic fractional ^{13}C labeling and two-dimensional NMR spectroscopy. *Metabolic Engineering.* 1, 189-197.

- Thevelein, J. M. (1994) Signal transduction in yeast. *Yeast*. 10, 1753-1790.
- Thevelein, J. M. and Hohmann, S. (1995) Trehalose synthase: guard to the gate of glycolysis in yeast. *Trends in Biochem. Sci.* 20, 3-10.
- Thevelein, J. M., Cauwenberg, L., Colombo, S., De Winde, J. H., Donation, M., Dumortier, F., Kraakman, L., Lemaire, K., Ma, P., Neuwalaers, F. R., Teunissen, A. Van Dijck, P., Versele, M., Wera, S. and Winderickx, J. (2000) Nutrient-induced signal transduction through the protein kinase A pathway and its role in the control of metabolism, stress resistance, and growth in yeast. *Enzyme and Microbial Technology*. 26, 819-825.
- Tomson, K., Barber, J. and Vanatalu, K. (2006) Adaptastat - a new method for optimising of bacterial growth conditions in continuous culture: Interactive substrate limitation based on dissolved oxygen measurement. *J. Microbiol. Methods*. 64, 380-390.
- Tran-Dinh, S., Bouet, F., Huynh, Q. and Herve, M. (1996) Mathematical models for determining metabolic fluxes through the citric acid and glyoxylate cycles in *Saccharomyces cerevisiae* by ¹³C-NMR spectroscopy. *Eur. J. Biochem.* 242, 770-778.
- Trumbly, R. J. (1992) Glucose repression in the yeast *Saccharomyces cerevisiae*. *Mol. Microbiol.* 6, 15-21.
- Vanatalu, K., Paalme, T., Vilu, R., Burkhardt, N., Junemann, R., May, R., Ruhl, M., Wadzack, J. and Nierhaus, K. H. (1993) Large-scale preparation of fully deuterated cell components. Ribosomes from *Escherichia coli* with high biological activity. *Eur. J. Biochem.* 216, 315-321.
- Varela, J.C., Praekelt, U. M., Meacock, P. A., Planta, R. J. and Mager, W. H. (1995) The *Saccharomyces cerevisiae* *HSP12* Gene Is Activated by the High-Osmolarity Glycerol Pathway and Negatively Regulated by protein Kinase A. *Mol. Cell. Biol.* Nov. 6232-6245.
- Vaughan-Martini, A. And Kurtzmann, C. P. (1985) Deoxyribonucleic acid relatedness among species of *Saccharomyces sensu stricto*. *Int. J. Syst. Bacteriol.* 35, 508-511.
- Verleur, N., Elgersma, Y., Van Roermund, C., Tabak, H. and Wanders, R. (1997) Cytosolic aspartate aminotransferase encoded by the *AAT2* gene is targeted to the peroxisomes in oleate-grown *Saccharomyces cerevisiae*. *Eur. J. Biochem.* 247, 972-980.
- Vinter, T., Paalme, T. and Vilu, R. (1992) "FermExpert" – an expert system for studies and optimization of processes of microbial synthesis. In: M. N., Karim and G. Stephanopolous (Eds.), *Modeling and Control of Biotechnical Processes*. Pergamon Press, Oxford, England, 467-470.
- Walker, T. E., Han, C. H., Kollman, V. H., London, R. E. and Matwiyoff, N. A. (1982) ¹³C Nuclear Magnetic Resonance Studies of the Biosynthesis by *Microbacterium ammoniaphilum* of L-Glutamate Selectively Enriched with Carbon-13. *J. Biol. Chem.* 257, 1189-1195.
- Weitzel, G., Pilatus, U. and Rensing, L. (1987) The cytoplasmic pH, ATP content and total protein synthesis during heat shock protein inducing treatments in yeasts. *Exp. Cell. Res.* 170, 64-79.
- Wiechert, W., Möllney, M., Isermann, N., Wurzel, M. and de Graaf, A. (1999) Bidirectional Reaction Steps in Metabolic Networks: III. Explicit Solution and Analysis of Isotopomer Labeling Systems. *Biotechnol. Bioeng.* 66, 69-85.
- Wiechert, W. (2001) ¹³C Metabolic Flux Analysis. *Metabolic Engineering*. 3, 195-206.

Wittmann, C., Hans, M., van Winden, W. A., Ras, C. and Heijnen, J. J. (2005) Dynamics of intracellular metabolites of glycolysis and TCA cycle during cell-cycle-related oscillation in *Saccharomyces cerevisiae*. 89, 839-847.

van Wuytswinkel, O., Reiser, V., Siderius, M. C., Kelders, G., Ammerer, H., Ruis, H. and Mager, W. H. (2000) Response of *Saccharomyces cerevisiae* to severe osmotic stress: evidence for a novel activation mechanism of the HOG MAP kinase pathway. *Mol. Biol.* 37, 382-397.

Zabriskie, T. M. and Jackson, M. D. (2000) Lysine biosynthesis and metabolism in fungi. *Nat. Prod. Rep.* 17, 85-97.

Zupke, C., Stephanopoulos, G. (1994) Modeling of isotope distribution and intracellular fluxes in metabolic networks using atom mapping matrices. *Biotechnol. Prog.* 10, 489-498.

ACKNOWLEDGEMENTS

This study is based on the work carried out at the Laboratory of Molecular Genetics of the National Institute of Chemical Physics and Biophysics, and Competence Centre for Food and Fermentation Technologies. The financial support from Estonian Targeted funding projects SF0222602Bs03 and SF0220378s98, and Estonian Science Foundation projects (Grants Nos. 5129 and 5160) is acknowledged.

I would like to express my sincere gratitude to all those people in both institutions who have supported my thesis research, specially my supervisor Prof. Toomas Paalme.

The help by Kerti Orumets and Mariane Koplmaa while making the fluorescence labeling experiments is greatly acknowledged.

Finally, I wish to thank my family and girlfriend for their understanding, patience and moral support.

APPENDIX I

Mass balance equations of the intermediates of *S. cerevisiae* during the growth on mixed substrates of glucose and acetate according to the Fig. 21 (Paper VI).

Intermediate	Mass balance equation
1. Glucose-6-P	$GLK1=PGI1+ZWF1+o_1$
2. 6-P-glyconolactone	$ZWF1=PGL1$
3. 6-P-glyconate	$PGL1=GND1,2$
4. Ribulose-5-P	$GND1,2=RK11+RPE1$
5. Xylose-5-P	$RPE1=TKL1,2a+TKL1,2b$
6. Ribose-5-P	$RK11=TKL1,2a+o_3$
7. Seduheptulose-7-P	$TKL1,2a=TAL1$
8. Erythrose-4-P	$TAL1=TKL1,2b+o_4$
9. Fructose-6-P	$PGI1+TKL1,2b+TAL1=PFK1,2+o_2$
10. Fructose-1,6-P	$PFK1,2=FBA1$
11. Dihydroxyacetone-P	$FBA1=TP11$
12. Glyceraldehyde-3-P	$TKL1,2a+TKL1,2b+FBA1+TP11=TAL1+TDH1,2,3+o_5$
13. 1,3-diphosphoglycerate	$TDH1,2,3=PGK1$
14. 3-P-glycerate	$PGK1=GPM1+o_6$
15. 2-P-glycerate	$GPM1=ENO1$
16. Phosphoenolpyruvate	$ENO1=PYK1,2+o_7$
17. Pyruvate _c	$PYK1,2=PC+PYC1,2$
18. Oxaloacetate _c	$PYC1,2=OAC+o_{10c}$
19. Pyruvate _m	$PC+MAE1=PDH1+o_{8m}$
20. Oxaloacetate _m	$OAC1+MDH1=CIT1,3+o_{10m}$

Analytical solution of the linear equation system, consist of the independent metabolic fluxes of *S. cerevisiae* during the growth on mixed substrate of glucose and acetate (Paper VI).

Flux	Analytical solution
ZWF1	$ZWF1 = -1/2(o_{11c} - o_{NADPHc} - X)$
PGL1	$PGL1 = -1/2(o_{11c} - o_{NADPHc} - X)$
GND1,2	$GND1,2 = -1/2(o_{11c} - o_{NADPHc} - X)$
RK11	$RK11 = -1/6(o_{11c} - 4o_3 - 2o_4 - o_{NADPHc} - X)$
RPE1	$RPE1 = -1/3(o_{11c} + 2o_3 + o_4 - o_{NADPHc} - X)$
TKL1,2a	$TKL1,2a = -1/6(o_{11c} + 2o_3 - 2o_4 - o_{NADPHc} - X)$
TAL1	$TAL1 = -1/6(o_{11c} + 2o_3 - 2o_4 - o_{NADPHc} - X)$
TKL1,2b	$TKL1,2b = -1/6(o_{11c} + 2o_3 + 4o_4 - o_{NADPHc} - X)$
PG11	$PG11 = -1/2(2o_1 - o_{11c} + o_{NADPHc} - 2qGLC + X)$
PFK1,2	$PFK1,2 = -1/6(6o_1 - o_{11c} + 6o_2 + 4o_3 + 2o_4 + o_{NADPHc} - 6qGLC + X)$
FBA1	$FBA1 = -1/6(6o_1 - o_{11c} + 6o_2 + 4o_3 + 2o_4 + o_{NADPHc} - 6qGLC + X)$
TP11	$TP11 = -1/6(6o_1 - o_{11c} + 6o_2 + 4o_3 + 2o_4 + o_{NADPHc} - 6qGLC + X)$
TDH1,2,3	$TDH1,2,3 = -1/6(12o_1 - o_{11c} + 12o_2 + 10o_3 + 8o_4 + 6o_5 + o_{NADPHc} - 12qGLC + X)$
PGK1	$PGK1 = -1/6(12o_1 - o_{11c} + 12o_2 + 10o_3 + 8o_4 + 6o_5 + o_{NADPHc} - 12qGLC + X)$
GPM1	$GPM1 = -1/6(12o_1 - o_{11c} + 12o_2 + 10o_3 + 8o_4 + 6o_5 + 6o_6 + o_{NADPHc} - 12qGLC + X)$

APPENDIX II

Yeast macromolecular composition, the concentration of individual monomers, and NADPH and NADH requirement for the biosynthesis. The fluxes to the biomass components are indicated as o_{nm} and o_{nc} referring to the n^{th} flux in the mitochondria or cytosol, depending on the enzyme localization determined from the ^{13}C labeling experiments.

Protein¹ (45 %)		NADPH	NADH	NADPH	NADH
<i>Monomers (o_i)</i>	Content in biomass [μmol g ⁻¹]	Content in biomass [mol mol ⁻¹]		Content in biomass [μmol g ⁻¹]	
Alanine (<i>o_{8m}</i>)	484.37	1	0	484.37	0
Arginine (<i>o_{11m}</i>)	124.75	4	-1	499.01	-124.75
Asparagine (<i>o_{10c}</i>)	75.74	1	0	75.74	0
Aspartate (<i>o_{10m}</i>)	247.08	1	0	247.08	0
Cysteine (<i>o₆</i>)	9.65	4	-1	38.61	-9.65
Glutamate (<i>o_{11m}</i>)	585.02	1	0	585.02	0
Glutamine (<i>o_{11c}</i>)	78.13	1	0	78.13	0
Glycine (<i>o₆</i>)	193.39	1	-1	193.39	-193.39
Glycine d (<i>o₆</i>)	193.39	1	-1	193.39	-193.39
Histidine (<i>o₃</i>)	70.96	4	-5	283.85	-354.81
Isoleucine (<i>o_{8m}</i> , <i>o_{10m}</i>)	238.38	5	0	1191.90	0
Leucine (<i>o_{8m}</i> , <i>o_{9m}</i>)	386.18	2	-1	772.37	-386.18
Lysine (<i>o_{9c}</i>)	341.17	3	-1	1023.50	-341.17
Methionine (<i>o_{10c}</i>)	10.87	5	0	54.33	0
Phenylalanine (<i>o₇</i> , <i>o₄</i>)	151.29	2	0	302.58	0
Proline (<i>o_{11c}</i>)	122.82	2	1	245.64	122.82
Serine (<i>o₆</i>)	108.83	1	-1	108.83	-108.83
Serine d (<i>o_{9c}</i>)	108.83	1	-1	108.83	-108.83
Threonine (<i>o_{10c}</i>)	211.72	3	0	635.16	0
Tryptophane (<i>o₇</i> , <i>o₄</i>)	20.81	3	-2	62.43	-41.62
Tyrosine (<i>o₇</i> , <i>o₄</i>)	74.77	2	-1	149.54	-74.77
Valine (<i>o_{8m}</i>)	330.93	2	0	661.87	0
Nucleic acids² (5.4 %)					
dAMP (<i>o₃</i> , <i>o₆</i>)	36.53	3	-3	109.6	-109.6
dGMP(<i>o₃</i> , <i>o₆</i>)	36.53	2	-3	73.07	-109.6
dUMP(<i>o₃</i>)	48.45	1	0	48.45	0
dCMP (<i>o₃</i>)	35.76	1	0	35.76	0
Lipids² (11 %)					
Lauric acid (<i>o_{9c}</i>)	130.70	10	0	1307.01	0
Palmitoleic acid (<i>o_{9c}</i>)	193.92	14	1	2714.86	193.92
Oleic acid (<i>o_{9c}</i>)	78.15	16	1	1250.39	78.15
Glycerol-P (<i>o₅</i>)	129.34	0	1	0	129.34
Poly- and disaccharides¹ (30 %)					
Glycogen (<i>o₁</i>)	232.25	0	0	0	0
Glucans (<i>o₁</i>)	422.89	0	0	0	0
Mannans (<i>o₁</i>)	914.36	0	0	0	0
Trehalose (<i>o₁</i>)	282.35	0	0	0	0

¹ Monomer concentrations determined directly from the biomass

² Monomer concentrations determined from the corresponding macromolecular fraction based on the relative concentrations according to Cortassa et al. (1995)

ARTICLE I

Drews, M., Kasemets, K., Nisamedtinov, I., Paalme, T. Continuous cultivation of insect and yeast cells at maximum specific growth rate

Reprinted from: Proceedings of Estonian Academy of Sciences, Chemistry. 1988, 47, p. 175-188

With permission from Estonian Academy Publishers

ARTICLE II

Kasemets, K., Drews, M., Nisamedtinov, I., Adamberg, K., Paalme, T. Modification of A-stat for the characterization of microorganisms

*Reprinted from: Journal of Microbiological Methods. 2003, 55, p. 187–200
With permission from Elsevier*

ARTICLE III

Nisamedtinov, I., Adamberg, K. and Paalme, T. D-stat

*Reprinted from: Proceedings of the 1st International Congress on Bioreactor Technology in Cell, Tissue Culture and Biomedical Applications. 2003, p. 231–242
With permission from BioBien Innovations*

ARTICLE IV

Drews, M., Nisamedtinov, I. and Paalme, T. Application of quasi-steady-state cultures

Reprinted from: Proceedings of the 1st International Congress on Bioreactor Technology in Cell, Tissue Culture and Biomedical Applications. 2003, p. 218–225

With permission from BioBien Innovations

ARTICLE V

Kasemets, K., Nisamedtinov, I., Abner, K. and Paalme, T. Study of the fermentative growth of *S. cerevisiae* S288C using auxo-accelerostat technique

Reprinted from: Modern Multidisciplinary Applied Microbiology: Exploiting Microbes and Their Interactions. 2006, p. 756–762
With permission from Wiley-VCH

ARTICLE VI

Paalme, T., Nisamedtinov, I., Laht, T. M., Drews, M. and Pehk, T. Application of (13)C-[2]- and (13)C-[1,2] acetate in labelling studies of yeast and insect cells

*Reprinted from: Antonie Van Leeuwenhoek. 2006, 89, p. 443–457
With permission from Springer Netherlands*

ARTICLE VII

Nisamedtinov, I., Lindsey, G., Karreman, R., Orumets, K., Koplmaa, M. and Paalme, T.
Effect of slowly increasing temperature and NaCl concentration on the expression of Hsp12-
Gfp2 fusion protein in *Saccharomyces cerevisiae*: an auxo-accelerostat study

*Reprinted from: Proceedings of the 2nd International Congress on Bioreactor Technology in
Cell, Tissue Culture and Biomedical Applications. 2006, in press
With permission from BioBien Innovations*

KOKKUVÕTE

¹³C- ja fluoressentsmärgise kasutamine *Saccharomyces* spp. ainevahetuse uurimisel

Käesolevas doktoritöös uuriti kahe erineva märgismeetodi kasutamist pärmiraku ainevahetuse uurimisel: 1) esimesel puhul toimus *S. uvarum* W34 biomassi märgistamine magneetiliselt aktiivset ¹³C-d sisaldavat Na-atsetaati ja märgistamata glükoosi sisaldaval segasöötmel, mille eesmärgiks oli visualiseerida rakus toimuvad ainevahetusrajad ning määrata rakus toimuvate ainevahetusreaktsioonide lokaliseerimine, kasutades lisaks veel ainevahetuse voogude mudelit; 2) teisel juhul uuriti madalamolekulaarset stressivalgu Hsp12p kodeeriva geeni ekspressiooni erinevatel, sujuvalt ja astmeliselt muutuvatel keskkonnatingimustel, kasutades nn. fluoressseeruvat märgist – rohelist fluoressseeruvat proteiini (Gfp2p) sünteesivat rakukonstrukti, kus *GFP2* ekspresseerub *HSP12* promootori kontrolli all. Eksperimentide läbiviimisel kasutati läbivoolukultuuride edasiarendusi, nagu D-staat ja aukso-akselerostaat.

¹³C-märgistuse eksperimentidega näidati ära, et rakusisesed ainevahetuse voogude väärtused on suhteliselt lihtsalt teoreetiliste mudelite abil arvutatavad, kui on teada rakus toimuvad võimalikud ainevahetuse reaktsioonid ning mõningate täiendavate voogude väärtused, nagu substraatide eritarbimiskiirused, produktide väljutuskiirused ning biomassi koostis. Märgise liikumise mustri valgust koostises olevatesse aminohapetesse ning arvutatud absoluutsetest ja tinglikest rikastustest selgus, et antud katsetingimustes toimusalaniini ning aspartaadi süntees mitokondris. NADPH bilanss rakus kinnitas ka seda, et biosünteesiks vajalik NADPH mitokondrites sünteesitakse *MAE1* reaktsiooni kaudu.

Katsetes fluoressentsmärgisega vaadeldi kahe levinud stressifaktori – temperatuur ning osmootne rõhk mõju *HSP12* ekspressioonile sujuvalt muutuvates tingimustes ning saadud tulemusi võrreldi nn. impulsskatsetega. Leiti, et *HSP12* ekspressioon stressitingimustes sõltub rohkem stressifaktori muutumise kiirusest kui konkreetsest stressifaktorist endast. Auksoostaate kultiveerimismeetodi edasiarendus aukso-akselerostaat sujuvalt muudetavate keskkonnaparameetritega, kasutades Hsp12p-Gfp2 konstrukti on efektiivne vahend uurimaks pärmiraku stressivastuseid erinevates, nii tööstuslikes kui looduslikes stressitingimustes.

CURRICULUM VITAE

Name	Ildar Nisamedtinov
Date of birth	07.10.1976
Place of birth	Tartu
Contacts	Competence Centre for Food and Fermentation Technologies (CCFFT), Akadeemia tee 15B, 12618 Tallinn, Estonia Tel: 6 408 202, Fax: 6 408 282 , e-mail: inisamedtinov@lallemand.com
Education	2002-2006 PhD studies, TUT, food and biotechnology 1999-2001 MSc studies, TUT, food and biotechnology 1994-1999 BSc studies, TUT, food and biotechnology
Employment	1997-1999 Engineer, National Institute of Chemical Physics and Biophysics, Laboratory of Molecular Genetics 2004- Research Project Manager, CCFT
Additional professional training	“Biomedical NMR” Apr. 15-19, 2003, Gothenburg, Sweden R&D laboratory of Lallemand, Inc., Sept.1999-Apr.2000, Montreal, Canada
Participation in scientific projects	Estonian Science Foundation Grants no: 5129, 5551 and 5160 “Stress optimization in yeast as a cell factory” (applied for targeted funding in October, 2006)
Research area	Metabolic studies of yeast <i>S. cerevisiae</i> , metabolic modeling, ¹³ C and fluorescence labeling, yeast stress responses, yeast as a cell factory
Membership	Member of Estonian Society for Microbiology

ELULUGU

Nimi	Ildar Nisamedtinov
Sünniaeg	07.10.1976
Sünnikoht	Tartu
Kontaktid	Toidu- ja Fermentatsioonitehnoloogia Arenduskeskus (TFTAK), Akadeemia tee 15B, 12618 Tallinn, Eesti Tel: 6 408 202, Fax:6 408 202, e-mail: inisamedtinov@lallemand.com
Hariduskäik	2002-2006 PhD, TTÜ, bio- ja toiduainete tehnoloogia 1999-2001 MSc, TTÜ, bio- ja toiduainete tehnoloogia 1994-1999 BSc, TTÜ, bio- ja toiduainete tehnoloogia
Teenistuskäik	1997-1999 Insener, Keemilise ja Bioloogilise Füüsika Instituut, Molekulaargeneetika labor 2004- Projektijuht, TFTAK
Täiendõpe	“Biomedical NMR” Apr. 15-19, 2003, Göteborg, Rootsi Lallemand, Inc. teadus ja arenduslabor, Sept.1999-Apr.2000, Montreal, Kanada
Osalemine teadusprojektides	Eesti Teadusfondi projektid nr.: 5129, 5551 and 5160 “Stress optimization in yeast as a cell factory” (esitatud sihtfinantseerimiseks okt., 2006)
Teadustöö põhisuunad	Pärmiraku (<i>S. cerevisiae</i>) ainevahetuse uurimine, ainevahetuse mudelid, ¹³ C- ja fluoressentsmärgised, rakus toimuvad stressindutseeritud metaboolsed vastused
Teadusorganisatsiooniline tegevus	Eesti Mikrobioloogide Ühenduse liige